University of Texas Rio Grande Valley
ScholarWorks @ UTRGV

Theses and Dissertations

12-2016

Study of selective laser remelting of 316L S.S. to reduce roughness on inclined surface

Jafar Ghorbani
The University of Texas Rio Grande Valley

Follow this and additional works at: https://scholarworks.utrgv.edu/etd

Part of the Manufacturing Commons

Recommended Citation

Ghorbani, Jafar, "Study of selective laser remelting of 316L S.S. to reduce roughness on inclined surface" (2016). *Theses and Dissertations*. 205.
https://scholarworks.utrgv.edu/etd/205

This Thesis is brought to you for free and open access by ScholarWorks @ UTRGV. It has been accepted for inclusion in Theses and Dissertations by an authorized administrator of ScholarWorks @ UTRGV. For more information, please contact justin.white@utrgv.edu, william.flores01@utrgv.edu.

STUDY OF SELECTIVE LASER REMELTING OF 316L S.S. TO REDUCE ROUGHNESS ON INCLINED SURFACE

A Thesis

by

JAFAR GHORBANI

Submitted to the Graduate College of
The University of Texas Rio Grande Valley
In partial fulfillment of the requirements for the degree of

MASTER OF SCIENCE ENGINEERING

December 2016

Major Subject: Manufacturing Engineering

STUDY OF SELECTIVE LASER REMELTING OF 316L S.S. TO REDUCE ROUGHNESS ON INCLINED SURFACE

A Thesis
by
JAFAR GHORBANI

COMMITTEE MEMBERS

Dr. Jianzhi Li
Chair of Committee

Dr. Rajiv Nambiar
Committee Member

Dr. Anil Srivastava
Committee Member

December 2016

Copyright 2016 Jafar Ghorbani

All Rights Reserved

ABSTRACT

Jafar, Ghorbani, Study of Selective Laser Remelting of 316L S.S. to Reduce Roughness on Inclined Surface. Master of Science Engineering (MSE), December, 2016, 83 pp., 14 tables, 46 figures, references, 53 titles.

Additive manufacturing (AM) technologies are increasingly competing with subtractive methods, and there are promising applications for additive technologies that are hybrid with traditional manufacturing methods. Poor surface roughness of additive manufactured parts continues to be a major challenge especially for advanced functional parts. In this study, effect of processing parameters are evaluated, optimized and verified by using the Box–Behnken design of experiment method. The results, for the first time, reveal that surface remelting has the potential to become a high speed approach for improving the roughness of non-horizontal surface of additive manufactured parts.

DEDICATION

To my wife, Mandana, wholeheartedly motivated, inspired, and supported me by all means to complete this program. Thank you for your endless love and patience.

ACKNOWLEDGMENTS

I would like to highly acknowledge Dr. Jianzhi Li, chair of my thesis committee, for all of his advice and supports during this research. My gratitude also goes to Dr. Rajiv Nambiar, Dr. Anil Srivastava and Dr. Alley Butler, Dr. Kye Hwan (Kevin), Edna Orozco Lee and Dr. Yang Yang. I am also grateful to Hector Arteaga, SEM lab staffs in particular Hilario Cortez and Edgar Munoz, materials lab staffs and other high-bay staff that supported me in different stages of my research. I am thankful to Manufacturing & Industrial Engineering department staffs including Elizabeth Rodriguez and Leticia Ocañas supports. I appreciate all my friends supports especially Josue Banuelos, Gabriel Rueda and Majid Hosseini. Special thanks to Robert Aguilar, Kevin Collier and Matthew Duffy from Renishaw Company for their technical advice for operating the machine.

TABLE OF CONTENTS

Page

ABSTRACT………………………………………………………….……….….. iii

DEDICATION……………………………………………………….………... iv

ACKNOWLEDGMENTS………………………………………….………. v

TABLE OF ONTENTS……………………………….……………...……... vi

LIST OF TABLES………………………………………………………………. ix

LIST OF FIGURES……………………………………………………….……… x

CHAPTER I. INTRODUCTION…………………………………….….……... 1

1.1 A brief background review…………………………….……..……. 1

1.2 Problem statement and Research Objectives ……………….…..………. 3

1.3 Overview of Research Methodology ……………………………………… 4

1.4 Organization of Thesis………………………………….……………. 4

CHAPTER II. REVIEW OF LITERATURE …………………...……..……… 6

2.1 Additive Manufacturing (AM)……………………………..……… 6

2.2 Selective Laser Melting (SLM)……………… ……………………..……. 7

2.3 Surface roughness as one of main limitation of AM……………………… 8

2.4 Optimization of process parameters ……………………….…………… 10

2.5 Prediction of the surface roughness ………………………...…..……….. 11

2.5.1 Prediction of the surface roughness of SLM parts ………………..… 13

2.6. Surface morphology analysis through SEM ………………….……………. 14

2.7 Post processing processes …………………………………..…………… 17

2.8 Hybrid manufacturing processes………………………………………. 18

2.9 Laser surface modification processes…………………………..…..……. 19

2.10 Laser polishing (LP) and additive manufacturing (AM)………...……… 23

CHAPTER III. METHODOLOGY…………………………………………………... 26

3.1 Materials …………………………………………….………………… 26

3.2 Selective Laser Melting System …………………………..…………..…. 27

3.3 Methods……………………………………………..……..………..….. 29

3.3.1 CAD file preparation ……………….…….…………….…..………….. 31

3.4 Surface roughness evaluation …………………………………..…………... 37

CHAPTER IV. RESULTS AND DISCUSSION……………………………………... 40

4.1 Experimental design and modeling ……………………………..…………. 40

4.2 Main effects of process independent variables on surface roughness ……..… 43

4.2.1 Effect of remelting layer thickness …………………………………… 44

4.2.2 Point distance effect…………………………………..……………… 45

4.2.3 Laser exposure time effect……………………………………………. 45

4.2.4 Laser power effect ………………………………………………..……. 45

4.3 Interaction plots for response……………………………………………. 46

4.4 Analysis of variance (ANOVA) and effect of input parameters……………. 47

4.5 Transformation necessity…………………………………………………… 56

4.6 Fitting Regression Model………………………………………………… 56

4.6.1 Regression Equation in Uncoded (actual) Units…………………….. 57

        4.6.2 Regression Equation in coded (dimensionless) Units………………. 58

    4.7 Validate model assumptions in regression or ANOVA……………………. 58

    4.8 Contour plots of response……………………………….……………….. 63

    4.9 Surface plots of response………………………………………………… 65

    4.10 Response Optimization………………………………………………… 71

        4.10.1 Validation of Optimization model………………………………….. 72

    4.11 SEM of surface………………………………………………………. 72

CHAPTER V. CONCLUSIONS AND FUTURE RESEARCH……………………… 77

REFERENCES……………………………………………………………………….. 79

BIOGRAPHICAL SKETCH……………………………………………………………. 83

LIST OF TABLES

Page

Table 3.1: Chemical composition (Weight %) of 316L stainless steel powder……… 26

Table 3.2: Technical specification of Renishaw AM 250 laser melting machine …...... 28

Table 3.3: Parameters and ranges for Box-Behnken design…………………….………. 30

Table 3.4: Relationship between slice thickness and number of slices …………..……… 35

Table 4.1: Box–Behnken design of experiments matrix and results…………………….. 42

Table 4.2: Analysis of Variance for surface roughness including all quadratic terms… 48

Table 4.3: Estimated Coded Coefficients for roughness including all quadratic terms… 49

Table 4.4: Analysis of Variance for surface roughness after removing term T*E…….. 50

Table 4.5: Estimated Coded Coefficients after removing term T*E…………………….. 51

Table 4.6: Analysis of Variance for surface roughness after removing term D*P…..…. 52

Table 4.7: Estimated Coded Coefficients after removing term D*P…………………… 53

Table 4.8: Analysis of Variance for surface roughness after removing term T*D……. 54

Table 4.9: Estimated Coded Coefficients after removing term T*D……………………. 57

Table 4.10: Variable setting and fitted response for optimized predicted solution…….. 72

LIST OF FIGURES

Page

Figure 2.1: Generic illustration of an AM powder bed system………………………….. 7

Figure 2. 2: Stair stepping effect ………………………………………………………… 12

Fatigue 2.3: Test part fabrication and measurement……………………………………….. 13

Figure 2. 4: SEM image of a horizontal surface…………………………………………… 15

Figure 2.5: SEM image of a slightly inclined surface …………………………………….. 16

Figure 2.6: Presence of particle on highly sloped surface (sloping angle 90)…………… 17

Figure 2.7: Overview of laser polishing …….…………………………………………… 22

Figure 3.1: SEM image of 316L austenitic stainless steel powder……………………….. 27

Figure 3.2: Renishaw AM 250 laser melting machine……………………………………. 28

Figure 3.3- 4x4 printed test series……………………………………………………… 29

Figure 3.4: Typical SLM printed sample based on Box-Behnken design………………… 31

Figure 3.5: Snapshot of creating 45 º inclined sample file in Magics® software…………. 32

Figure 3.6: Dimensions and geometry of 45 º inclined sample file ……………………….. 32

Figure 3.7: Snapshot of creating 45 º inclined remelting layer file in Magics® software…. 33

Figure 3.8: Dimensions and geometry of 45 º inclined thin layer file in Magics® software 34

Figure 3.9: Scan strategy in Renishaw build processor slice viewer…………………….. 34

Figure 3.10: Manual metallurgical sample mounting press…………………..…………… 36

Figure 3.11: Some of samples after mounting process…………………………………….. 37

Figure 3.12- roughness measuring instrument set up…………………………………… 38

Figure 3.13: A sample of roughness measurement on not remelted (initial) surface……. 38

Figure 3.14: A sample of roughness measurement on remelted (final) surface…….……. 39

Figure 3.15: scanning electron microscope set up…………………………………….. 39

Figure 4.1: Main effects plot for response (fitted means)……………………………….. 43

Figure 4.2: Interaction plots for response (fitted means)……………………………… 46

Figure 4.3: Residual plots for response (Surface roughness)…………………………… 59

Figure 4.4: Residual versus variable T (Remelting layer thickness)…………………….. 60

Figure 4.5: Residual versus variable D (point distance)………………………………. 60

Figure 4.6: Residual versus variable E (laser exposure time)…………………………….. 61

Figure 4.7: Residual versus variable P (laser power) …………………………………….. 61

Figure 4.8: Normal probability plot of residual- 95% CI………………………………. 62

Figure 4.9: Scatter plot of surface roughness (response variable)…………………………. 63

Figure 4.10: Contour plots at minimum set of hold values……………………………….. 64

Figure 4.11: Contour plots at average set of hold values………………………………. 64

Figure 4.12: Contour plots at maximum set of hold values………………………………. 65

Figure 4.13: three-dimensional surface plot of surface roughness versus P and E………. 66

Figure 4.14: three-dimensional surface plot of surface roughness versus P and D………. 67

Figure 4.15: three-dimensional surface plot of surface roughness versus D and E………. 68

Figure 4.16: three-dimensional surface plot of surface roughness versus T and P………. 69

Figure 4.17: three-dimensional surface plot of surface roughness versus T and E………. 70

Figure 4-18:three-dimensional surface plot of surface roughness versus T and D………. 70

Figure 4-19:- response optimization plot………………………………………………. 71

Figure 4-20: SEM image of run 4 sample at magnification 100 ………………………… 73

Figure 4-21: SEM image of run 1 sample at magnification 100………………………….. 74

Figure 4-22: SEM image of run 4 sample at magnification 400 …………………………. 75

Figure 4-23: SEM image of run 1 sample at magnification 400 ………………………….. 75

Figure 4-24: SEM image of central area of run 1 sample at magnification 400 ………… 76

CHAPTER I

INTRODUCTION

The main objective of this chapter is to provide an introduction and overview about this study. The problem description, research purposes, overall research methodology and finally the structure of the thesis are covered in this chapter.

1.1 A brief background review

Selective laser melting (SLM) is one of the main subcategories of additive manufacturing (AM) technology which is increasingly being used for end-user functional metallic parts (Gibson et al, 2014). Higher geometrical freedom, powder-based additive technology, manufacturing remarkably low porosity parts and printing customized parts with complex structure expanded SLM application for manufacturing advanced functional metallic components mainly in biomedical, aerospace, and automotive sectors (Bourell, 2016). In spite of numerous competitive advantages of SLM process, desirable surface quality and dimensional accuracy are the main challenges for expanding SLM application especially for highly loaded and surface sensitive parts (Gu et al., 2012). In practice, post-processing methods including mechanical, thermal, and chemical processes can be exploited to improve surface quality, however these methods are time consuming and not environmental friendly (Braga et al., 2007). From the engineering perspective, surface roughness plays a crucial role in many functional parts. Rough surface could initiate cracks and eventually decrease parts' performance in fatigue, corrosion and tribology, especially when they are exposed to dynamic loads during lifecycle of engineering parts (Mumtaz & Hopkinson, 2009). In traditional subtractive techniques including milling process, Ra values of less than 1 μm are obtainable. However, for SLM manufactured parts, these values generally vary between 2 and 20 μm depending on powder characteristics, the process parameters selected and scanning strategies used. During last decade, laser technology has been developed to a level that it can be considered as an appropriate tool for polishing or modification of surface of metallic components to enhance topographic, esthetic, and functional properties of component surfaces (Bordatchev et al., 2014).

Since the energy source of selective laser melting and laser polishing is the same, the hybrid selective laser melting and laser polishing (re-melting) could be very attractive to enhance surface quality with little production time loss. Nowadays, laser surface re-melting (LSR) method is widely used to decrease either the surface roughness or volumetric porosity in SLM process. In addition, it was incorporated as an option in many additive manufacturing software including Magics®. However, most of the studies focused on the improvement of horizontal surface roughness though large portion of parts surfaces are inclined (Kruth et al., 2008).

Vaithilingam et al. (2016) demonstrated that surface remelting could negatively change the surface chemistry by selective evaporation of susceptible alloying elements. They attributed this phenomenon to the remarkably high energy density which the remelting process induces on the surface layers of the part, due to the unique surface laser scan techniques used in most remelting processes. Therefore, this limitation should be considered while applying skin scanning on any metallic alloy. Kruth and Yasa (2011) optimized laser process parameters and applied selective laser erosion / selective laser remelting on horizontal surfaces of 316L stainless steel and Ti-6Al-4V titanium alloy parts, improved Ra values from 15 μm to 1.5 μm and from 14.1 μm to 3.1 μm respectively. Wang et al. (2016) improved horizontal surface roughness of 316L stainless steel pars from Ra: 14.33 µm to Ra: 3.34 µm at best scenario.

Yasa and Kruth's study (2011) demonstrated that laser remelting could improve the surface roughness of curved and inclined surfaces as well. However, their technique revealed sharp rough area (bands) where two adjacent laser passes overlap each other. In addition, the minimal roughness that they obtained on an inclined surface was 5.18µm. Alrbaey et al. (2014) combined laser remelting as a post-processing tool with the selective laser melting process for optimizing the roughness of inclined surfaces and achieved the best result of 1.4 µm. This study proposed, analyzed and eventually optimized surface roughness of 45˚ inclined surface by printing a virtual thin shell on the base samples surfaces. This easy approach has the ability to improve initial surface roughness of Ra from more than 10 µm to less than 1 µm at a proper speed with minimum detrimental effect of part dimensional accuracy.

1.2 Problem Statement and Research Objectives

Surface roughness has been a real challenge for increasing selective laser melting process applications especially into functional parts that function under dynamic loads. During last decade most of the investigation for improving SLM manufactured metallic parts have been conducted on horizontal (top) surfaces. There are a few published studies on inclined surface roughness and the best reported surface roughness result were more than 1.5 µm (Kruth and Yasa, 2011). Therefore, the goal of this study is to evaluate the effects of selective laser melting process parameters on the surface roughness of inclined surfaces after applying surface remelting. Investigated parameters are laser power, laser exposure time, remelting layer thickness, and point distance. A design of experiment approach is utilized to model process for achieving optimum surface roughness.

1.3 Overview of Research Methodology

For this study, first four input processing parameters of selective laser melting, including laser power, laser exposure time, point distance, and remelting layer thickness were chosen. Then Bok-Bhenken method of response surface methodology is implemented to investigate effects of these parameters on surface roughness as design response surface. Twenty seven tests were run, then all surface underwent surface remelting. Finally, results were analyzed by the use of statistical analysis techniques and scanning electron microscope instrument.

1.4 Organization of Thesis

The whole structure of this study is made up of five chapters. Chapter one is introductory chapter of this thesis. It consists of a problem description statement, research main goals, general research methodology and finally this thesis content.

Chapter II is a brief review of the recent related literature. This includes additive manufacturing (AM) technologies classification, selective laser melting (SLM) principles, and why surface roughness is one of main limitation of AM. In addition, optimization of SLM process parameters and prediction of the surface roughness of SLM parts are discussed briefly. Recent literature on surface morphology analysis through SEM, post processing processes, and hybrid manufacturing processes are reviewed. Laser surface modification processes, application of laser polishing in additive manufacturing, and laser polishing of selective laser melting are discussed at the end of this literature review chapter.

Chapter III deals with design of experiments, materials and methods used in this study. Raw material specification, system technical specification, process parameters set-up are explained and finally, instrumentation and tools used for measuring surface roughness are explained at the end of this chapter.

Chapter IV provides results from the designed experiments. A step by step statistical analysis with relevant tables, graphs, and detailed discussion are covered based on a design of experiment methodology.

Lastly, chapter V. Summarizes conclusions of this research and recommends some topics for future studies on this field.

CHAPTER II

REVIEW OF LITERATURE

This chapter outlines a general classification of additive manufacturing technologies and also more detail of power-bed based additive manufacturing especially selective laser melting (SLM) technique. Advantages and limitation of SLM are discussed to some extent. Then, surface roughness as one of main challenges of AM and optimization of AM process parameters is discussed. Additionally, prediction of the surface roughness especially on SLM parts and evaluation of surface morphology by SEM are reviewed. Post polishing processes and hybrid manufacturing processes as two of the main tools for roughness improvement are then discussed. This chapter will be completed by reviewing of studies on surface modification methods including laser polishing on selective laser melting (SLM) parts.

2.1 Additive Manufacturing (AM)

Historically, subtractive and formative manufacturing have been two dominant categories of manufacturing processes over at least last three centuries. Generally, subtractive manufacturing creates finished parts from raw bulk materials by use of traditional tools such as turning, milling, grinding and so on. Additionally, in formative manufacturing such as forging and casting, solid materials and molten materials respectively, are being used to produce parts via predefined molds and dies (Yoon et al., 2014). Recently, a new category of prototyping (and eventually manufacturing) technology has been emerged as additive manufacturing (also commercially known as 3D printing) for making prototypes, tools and even functional parts (Herzog et al., 2016).

Even though this technology is new, metal additive manufacturing has been transitioning from a pure rapid prototyping technology to a widespread technology whereby functional parts could be manufactured even for highly critical applications. In other words, ever since its development in the 1980s, additive manufacturing (AM) (Rapid Prototyping as it was originally called), has emerged as a powerful facet of advanced manufacturing. The principle of AM is that the part is created through layer-by-layer deposition of the desired material. The term Additive Manufacturing (AM) has been defined by ASTM International Committee F42 in (ASTM F2792-12a, 2012) as “process of joining materials to make objects from 3D model data, usually layer-upon-layer, as opposed to subtractive manufacturing methodologies, such as traditional machining” (Boschetto & Bottini, 2015). This standard for terminology established a classification of AM processes into seven main categories as follows:

1) Binder jetting
2) Directed energy deposition
3) Material extrusion
4) Material jetting
5) Sheet lamination
6) Vat polymerization
7) Powder bed fusion

Indeed, powder bed fusion is one of the widely used AM technologies which have been implemented for producing of prototypes and also near net shape final products without geometrical intricacy restrictions (Boschetto & Bottini, 2015). In general, powder bed is prepared by evenly distribution of powder particles on a substrate. The energy source (electron beam or laser beam) is programmed to transfer energy to the surface of the bed melting or sintering the powder into the required shape. Additional powder is piled up across the work area, and the process is continued to create a solid 3D component. The advantages of this system include its ability to produce high resolution features, internal passages, and maintain dimensional control (Frazier, 2014). Figure 2.1 schematically represents a generic powder bed fusion system.

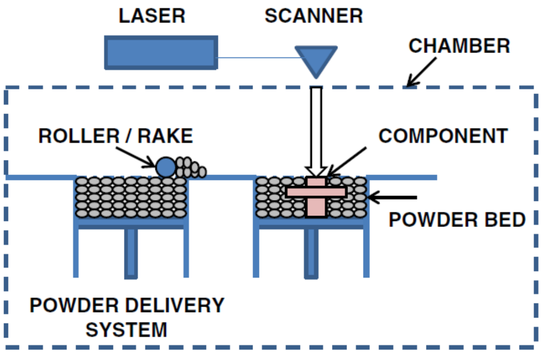

Figure 2-1- Generic illustration of an AM powder bed system (Frazier, 2014)

It has been estimated that for direct metal fabrication by additive manufacturing, powder bed fusion technology have the most commercial applications. These days, more focus is on the design and manufacturing of powder-bed fusion additive laser machines with smaller spot size and higher power for improving the surface roughness and also the built rate (King et al., 2014).

2.2 Selective Laser Melting (SLM)

Selective laser melting is a powder-based, additive manufacturing process where 3D part is manufactured, layer-by-layer, by utilizing a laser beam to completely melt and then solidify the metallic powder particles (Jia, & Gu, 2014). A particular challenge in this process is the selection of appropriate process parameters that result in parts with desired properties (Kamath et al., 2014).

Additive manufacturing techniques especially selective laser melting are very interesting for fabricating biomedical devices and parts for aerospace industries. Increasingly it is penetrating to other industries including automotive. Despite of many advantages of SLM process, such as the flexibility of choosing materials and the increased functional performances, there are still limitations, with poor surface finish as one of the most important one (Strano et al., 2013).

2.3 Surface roughness as one of main limitation of AM

The surface roughness and resolution of a part are critical in many engineering applications. Some applications need a surface roughness of about 0.8μm or lower to prevent initiated cracking of surfaces. Specifically, additive manufacturing has enabled the fabrication of complex parts and components using a layer-by-layer based method but it often produces parts whose roughness and tolerance are less desirable due to the nature of the process that involves melting and cooling the powders. Commercial powder bed machines such as MTT's realizer, EOS M270, etc. often need post processing operations such as surface machining, polishing and shot peening to enhance the final part finish surface. From the first commercialization of rapid prototyping in the late 1980, it was clear that due to layer by layer manufacturing nature of this new technology, inferior surface quality was one of main limitations of applying additive manufacturing in comparison to traditional subtractive technologies. However at that time priority was on expanding advantages of this systems rather than decreasing of relevant drawbacks (Yasa & Kruth, 2011).

With recent development in additive manufacturing technologies, especially during last decade, researchers on this ground considered surface quality of parts which are being manufactured by this new technology as a real challenge which could somewhat limit the advanced industrial applications of the process. A large stream of research has tried to investigate and improve surface roughness. For power bed fusion systems, it can be deduced from trend of recent publications that generally three major approaches have been considered by researchers, and these are optimization of independent parameters, application of post processing processes and also implementation of hybrid processes (Lavvafi, 2013). The hybrid approach (integration of additive and subtractive process) works by combining the best engineering aspects of additive processes (i.e. near-net shape parts) and subtractive processes (i.e. better geometric accuracy and surface finish) (Merklein et al., 2016).

In conclusion, AM provides the capabilities to process an ever-growing range of materials and produces parts with complex geometries without the additional cost and time associated with making fixtures, dies and tools (as in conventional manufacturing). However, when compared to conventional methods (subtractive methods such as machining), current AM methods produce parts with poorer surface finish and part accuracy. These aspects are not critical factors in certain applications such as biomedical implants where rougher surfaces are preferred to accelerate bone ingrowth. However, for most mechanical and aerospace applications, superior surface finish and part accuracies are desired. Hence, there is a need to solve two major challenges in AM which are increasing part accuracy and improving surface finish. As mentioned earlier, the fundamental approaches in addressing these challenges are to:

(1) Improve the performance of each AM processes and/or

(2) Application of post processing techniques and/or

(3) Develop a hybrid process

The first and second approaches are relatively challenging and time-consuming since there are multiple AM processes with unique processing techniques and characteristics such as energy source (laser, electron beam), processing nature (binder jetting, material powder bed fusion), etc. Hybrid processes incorporates AM methods as a pre-cursor where near-net AM-made parts can be coupled with conventional material removal processes such as machining. In order to improve the process performance of each AM method, discrete research efforts targeted at specific AM technologies are required (Karunakaran et al., 2010).

2.4 Optimization of process parameters

Some studies tried to optimize relevant materials, laser and operation interrelated parameters and understand details of mechanisms behind the creation of surface roughness. Yadroitsev et al. (2007) indicated that there are more than 130 parameters that could affect the final quality of the material that is being produced by laser powder-bed fusion additive manufacturing (AM) method. These include laser power, scan speed, scan-line spacing (hatching distance), powder layer thickness, scanning strategy, atmosphere, and powder bed temperature and so on, though these parameters have different levels of importance. Lavvafi et al. (2012) demonstrated that the laser parameters will affects not only the roughness of the resulting surfaces, but also the depth of the heat affected zones on the surface of the alloy. Using a novel method to vary the surface roughness of the alloy, it is possible to improve the fatigue properties of the alloy. Lavvafi et al. (2012) showed that the fatigue properties of laser treated 316 stainless steel can improve significantly due to creation of fine-grains on the surface of the alloy, which consequently results in improved surface hardness, and therefore the fatigue life of the components.

Singhal et al. (2009) determined optimum part deposition orientation for achieving minimum average part surface roughness, minimum build time and support structure for selective laser sintering (SLS) processed parts by solving a multi-objective optimization problem. Recently a few researchers directly and deeply investigated the effects of build angles in AM and proposed theoretical models for the prediction of surface roughness for selective laser sintering process in order for the surface roughness of layered manufacturing processed parts to be predicted and controlled and eventually to alleviate the process from the need of the post processing step (Wang et al., 2016). It is generally accepted that NC-machined parts have superior surface quality than layered manufacturing parts. The stair-stepping effect and balling effect are among important factors that have more deleterious effects on surface quality of AM processed components so a comprehensive review of the factors that affect surface finish will be discussed in more detail in the following sections.

2.5 Prediction of the surface roughness

Ahn et al. (2009) considered the stir step phenomenon and mathematically modeled surface roughness. Figure 2.2 schematically shows concept of stair stepping effect in additive manufacturing processes. Theoretical CAD models have no surface roughness, but due to the fact that the object is created by a pile up of 2D layers, one on top of each other, inevitably leads to the stepping effect on the part surface. Figure 2 in fact simply shows that surface roughness can be decreased by reducing the 2D layer thickness, but unfortunately smaller layer thickness increases the manufacturing time. Indeed, this phenomenon has a great effect on surface quality. Therefore, understanding surface angle effects on surface roughness are of interest. According to this figure the main factors that influence the surface roughness are the layer thickness (L), surface angle (Θ), and surface profile angle (φ).

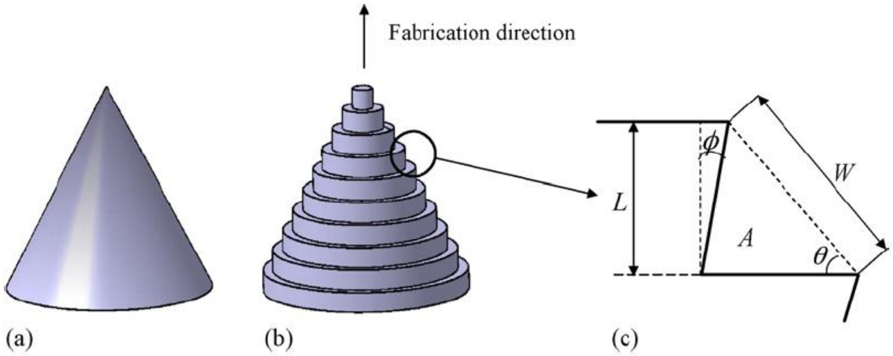

Figure 2. 2- Stair stepping effect in: a) CAD model, b) AM part, c) Surface profile Schematic (Ahn et al., 2009).

Figure 2.3 displays samples that were used for examining the effects of surface angle. This "truncheon" test part was designed to measure roughness surfaces inclined to the horizontal at "sloping angles" in the range 0^0–90^0 at 5^0 intervals and it allows the surface roughness for each inclination angle to be easily measured.

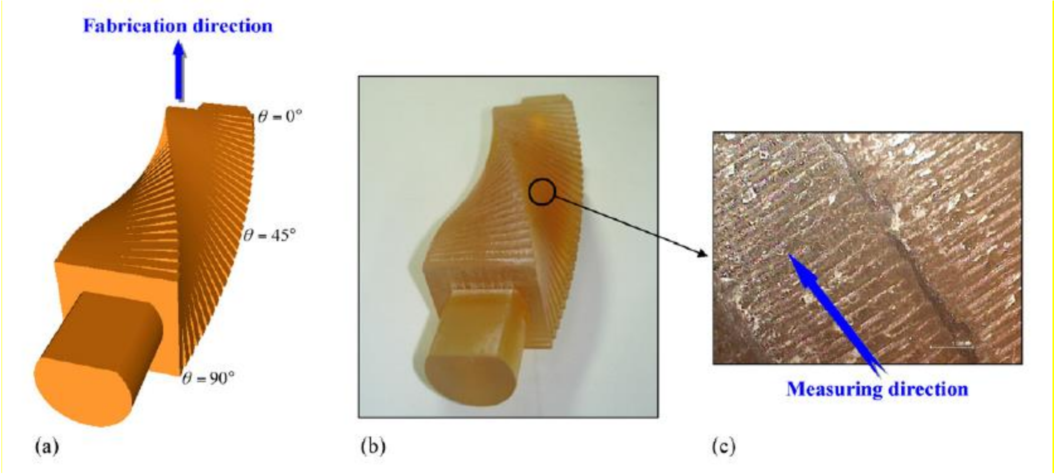

Fatigue 2.3- Test part fabrication and measurement: a) CAD Model, b) fabricated test part, c) magnification photograph of the surface (Ahn et al., 2009).

2.5.1 Prediction of the surface roughness of SLM parts

Strano et al. (2013), based on comparison of observed data, surface analysis and experimental data with previous models, indicated that in addition to geometrical considerations, for accuracy of a model, presence of some rough solidified particles on the surfaces at specific range of angles also should be considered in relevant mathematical modeling. Through analysis of the surface morphology and roughness at different inclinations of the upward surfaces of SLM parts, they identified the major effects and proposed a new mathematical model to predict the characteristics of the surface created through the SLM process. A surface roughness-sloping angle curve was also presented, which showed the variation in average surface roughness with different sloping angles. The horizontal surface (0^0 inclination) had lowest roughness, as expected. Surface roughness at 0^0 horizontal surface is caused due to the rippling effect that occurs during the laser melting process. It is concluded that when the laser moves, there is a temperature gradient between the laser beam and the solidifying zone, which generates a shear force on the liquid surface that is counter acted by surface tension forces. The gravity and surface curvature counteract the external shear force, thus tending to restore the surface height of the melt pool to the free level. However, due to the short melt pool solidification time, this relaxation process is often not fully achieved instead a residual rippling on the surface is formed. It has been shown (Strano et al., 2013) that it is possible to reduce the roughness generated by rippling effect, by surface remelting. As the inclination angle increases from 0^0, additional surface roughness is expected, resulting from the stair-step effect. It is important to notice that on the slanted surfaces, unlike on horizontal ones, laser remelting is not possible with SLM technology, since the material can only be sintered horizontally. The trend of roughness is always constant in the range of about 5^0–45^0, with a relatively slow decrease in the range of about 50^0–90^0.

2.6 Surface morphology analysis through SEM

Strano et al., (2013) compared SEM pictures of a horizontal surface (normal to the build direction) with a small inclination (5 degree) at 3 different magnifications (Figures 2.4 and 2.5). For the horizontal surface (Figure 2.4), there are very few sparse, partially-sintered particles on the surface, because of the small layer thickness (20μm) and the high power (195W) of the scanning laser beam which allow the powder to fully melt and fuse into a relatively smooth and uniform layer. The effects of scan direction and strategy such as hatch distance (highlighted by the arrows) are visible. For each scan line there are noticeable bullet-shaped marks oriented in accordance with the moving laser beam, presumably caused due to slower cooling in the center of each track.

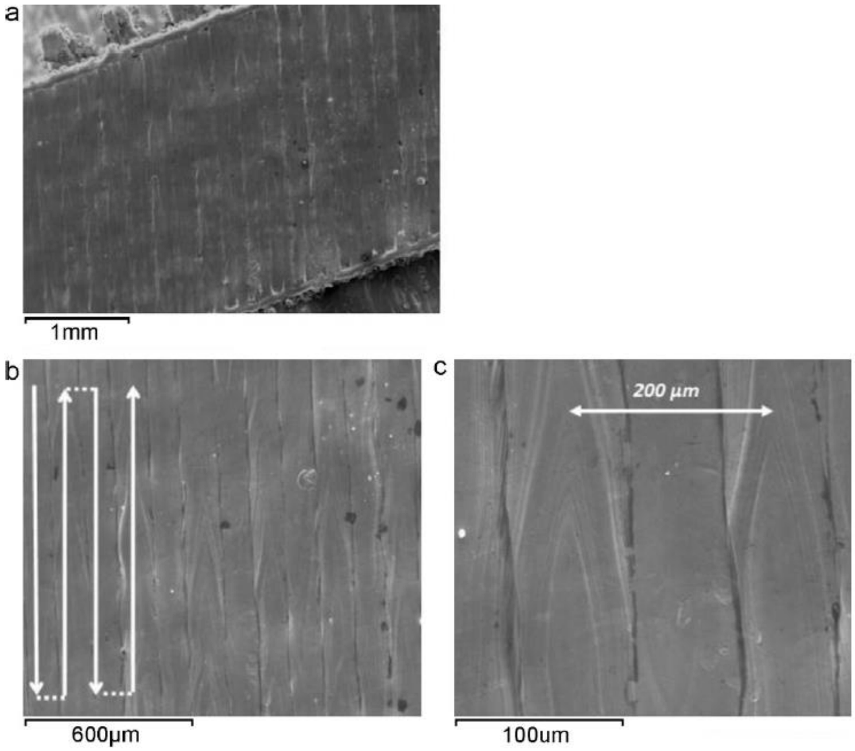

Figure 2. 4- SEM picture of a horizontal surface: a) an surface overview, b) detail profile, c) detail profile at high magnification (Strano et al., 2013).

As for the inclined surface (Figure 2.5) the stair-step is visible at intervals of about 230 μm.

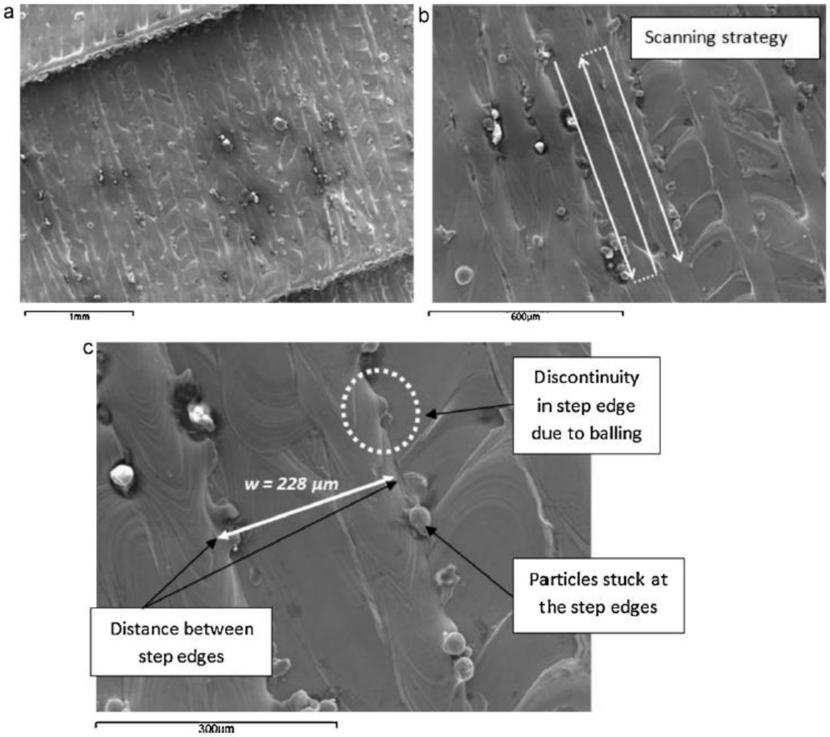
a
b
Scanning strategy
1mm
600µm
c
Discontinuity in step edge due to balling
w = 228 µm
Particles stuck at the step edges
Distance between step edges
300µm

Figure 2.5- SEM picture of a slightly inclined surface (sloping angle 5): a) at low magnification b) at high magnification, c) detail of slightly inclined surface (Strano et al., 2013).

When the build inclination increases, the SEM micrographs show the lack of sharpness of the step edges, due to discontinuities along step edges and the presence of partially bonded particles stuck at the edge borders. The formation of discontinuous borders is partially caused by the balling effect that happens during the laser melting of the metal powder. Balling is the breakup of the molten pool into small entities. During the laser melting of metal powders, the high thermal gradient between different volumes of the molten material generates a difference in surface tension within the pool, which produces Marangoni convection (Strano et al., 2013). Figure 2.6 shows a particular effect on the 90^0 inclined surface, a high number of partially bonded, clustered particles is present on the surface, and partially bonded particles can be considered the main cause of surface roughness at 90^0.

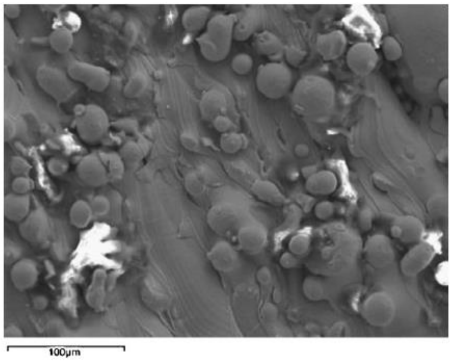

Figure 2.6- Presence of particle on highly sloped surface (sloping angle 90) (Strano et al., 2013).

2.7 Post processing processes

Additive manufacturing technologies rarely produce fully finished (net shape) parts specified by the customer requirement and part functions. Generally, after manufacture of the component via a specific AM process, for example for powder bed fusion system, tasks such as removal of residual powder particles, support scaffolding removal, further UV exposure for polymeric parts, heat treatment for reducing residual stress and/or improving mechanical properties reduce surface roughness and so on are required. Also, post processing has always been considered to be one of the practical ways to decrease surface roughness. Conventional polishing operations such as abrasive or electrochemical techniques are frequently used to decrease surface roughness. Apart from increasing of production time, these post processing activities have several limitations. Indeed, one of outstanding advantages of powder bed fusion additive manufacturing, similar to other additive techniques, is the ability to produce parts with high geometrical complexity. Therefore post processes such as abrasive process have a lot of difficulty to access interior surfaces of complicated parts. The electrochemical polishing process utilizes chemical materials and so has some problems especially from the environmental point of view (Rosa1 et al., 2015).

Rossl et al. (2015) studied the effect of several surface treatments including grinding and emery polishing to decrease surface roughness of the prototyped parts and reported that electroless nickel coatings after shot peening and polishing can considerably improve surface quality and corrosion resistance. It should be noted that though during post processing stage of AM technologies it is possible to improve surface roughness and accuracy of AM manufactured parts, for some applications such as fabricating die or mold using additive processes, it not a practical step. For example, dies and tool steel parts have around 60HRC hardness, and manual polishing them is a really rough and time consuming job (Löber et al., 1995).

2.8 Hybrid manufacturing processes

The third approach employs AM to produce near-net parts and then incorporates a ‘hybrid strategy’ to improve part accuracy and surface finish. Hybrid manufacturing processes play a crucial role by concurrently utilizing both a subtractive and an additive technique in order to improve the performance (Lauwers et al., 2014). Several investigators have identified the need for secondary operations and the advantages of coupling AM and machining methods. Chu et al., (2014) listed a total of fifty seven micro and nano scale hybrid manufacturing processes based on process timing and process type. In Chu et al., (2014) classification approach, the process type is defined as either geometrically additive or subtractive, and all hybrid processes are classified into combinations of additive, subtractive, and assistive process. It is reported that combination of direct metal laser sintering with high speed milling, electro discharge machining can be a good solution for prototype injection molds for plastic parts (Mognol, 2006).

Essentially, hybrid strategies have been developed for specific AM methods where additive and subtractive operations are repeated in a cyclic manner until the final part is created. However, in AM processes that are categorized as powder bed fusion processes, where the material is spread across in each layer, such hybrid strategies are not feasible. Hence, it is more efficient and rational to develop a hybrid strategy which is versatile and independent of any AM process characteristics. Such hybrid process needs to be consolidated yet adaptable to combine any near-net AM process with conventional SM process (Karunakaran et al., 2010). Successful development and implementation of such a hybrid process can accelerate the applications of AM-made parts and efficiently incorporate functionality such as part accuracy and surface finish (e.g. assembly sub-parts). In response to the aforementioned needs, laser polishing as a non-traditional subtractive method was studied by researchers, through integrating the hybrid power bed fusion process with the laser polishing post process with the aim to reduce limitations of power bed fusion technology.

2.9 Laser surface modification processes

Laser surface polishing, laser surface texturing and laser surface hardening are among the main laser surface modification processes that are being applied for a variety of purposes including but not limited to overcoming porosity issues, improving mechanical properties ranging from strength, corrosion resistance, wettability, micro-hardness, wear behavior, and fatigue. The reduction of surface asperities results from the volumetric redistribution of molten material under the influence of surface tension followed by rapid solidification. The laser polishing process has been applied successfully for more than a decade to reduce surface roughness of non-metal parts such as optical glasses or silicon wafers. This process is based on controlled melting and solidification of a thin layer of material close to surface. Unlike glasses, finishing could be time and cost-consuming in the manufacturing of several metal components, as the final morphology plays a fundamental role since it can influence both the visual appearance and working performance of several end-products (Park & Lee, 2009).

Surface finishing operations are a key step in a variety of industry sectors, namely die and mold industry, semi-conductor manufacturing, medical implants, and optical industry and so on. Whether it is for its tribological behavior, biocompatibility or optical response, the topography of a part can be of utmost importance. Traditional surface finishing techniques include material removal by abrasive processes, normally in a sequence of different steps, using wheels, vibrating tools or cloths, as well as chemical-mechanical polishing and electrochemical polishing. Disadvantages of these approaches include high manufacturing time and cost, for example, up to 30% of the total production cost in die and mold industry, dimensional deviations among different operators and high consumable cost. To circumvent these issues, polishing by laser radiation appears as an attractive alternative, worth evaluating. As in all laser based methods, laser polishing is a non-contact process, which can be automated with relative ease, and is therefore able to tackle complex, three-dimensional parts with precision and repeatability. In the late 1990, laser polishing only had been used for applications with high added value, such as optical industry, but nowadays it becomes increasingly applicable for metallic parts surfaces, with remarkable performance as a finishing process. Laser polishing possesses extra advantages for additive manufacturing techniques in that since both process works based on laser as a source of thermal energy so combining of these two additives and subtractive process is highly desirable. Laser polishing is one of the fast growing laser surface modification process that is expected eventually to replace current time consuming and costly manual polishing operation of especially metallic parts. It would be even more beneficial for complicated parts and also harder parts such as die and mold parts for which manual polishing is a major problem. Additionally, there is no contact between polishing tool and work piece, and there is no tool wear in comparison to conventional machining.

In general, the principle of laser polishing for metallic parts is melting a thin layer of material close to surface through laser irradiation. At the micro level, laser induced energy melt peaks of surfaces and this melted liquid filles in valleys of surface, thus reducing surface roughness (Lamikiz et al., 2007). Laser polishing process may be classified into two main categories: macro polishing and micro polishing. Macro polishing is carried out with continuous wave (cw) laser radiation. The best results achieved yet is the reduction of the roughness of a turned tool steel (DIN 1.2343) from Ra=5µm to Ra=1µm. In contrast to macro polishing, micro polishing is carried out with pulsed laser radiation. The range of pulse duration is 20 to 1000 ns and the remelting depth is about 0.5µm. Due to the small remelting depth, laterally larger surface structures remain unaffected, and, therefore, cannot be eliminated. The most important process parameters are pulse duration and intensity. Longer pulses generate higher pick laser power, thus possible to eliminate laterally larger surface structures. In most case, a top-hat intensity distribution is preferable to generate a homogenous remelting depth. Typical laser types used include Fiber-coupled Nd/YAG and excimer lasers with achievable processing time less than 3 s/cm^2. The correct selection for laser type depends on the initial roughness and surface homogeneity. In general, for values of the Ra parameter greater than around 0.5µm, the macro polishing is preferred. A sequential combination of both approaches is also possible, as demonstrated, for example, where an AISI H13 surface with a starting aerial topography roughness, Ra, of 1.35µm is laser smoothed down to 0.18µm. One of the first applications of the technique, in the late eighties and early nineties, termed planarization at the time, was in the field of microelectronics, to flatten out the surface of thin metal layers in integrated circuits and fill holes. Since then, several authors have demonstrated the potential of the technique on tool steels, stainless steel, titanium alloys, sintered bronze substrates, optical glasses, and ceramics. Figure 2.7 somewhat clarifies concept of relocation of thin layer at surface of metallic material due to laser irritation.

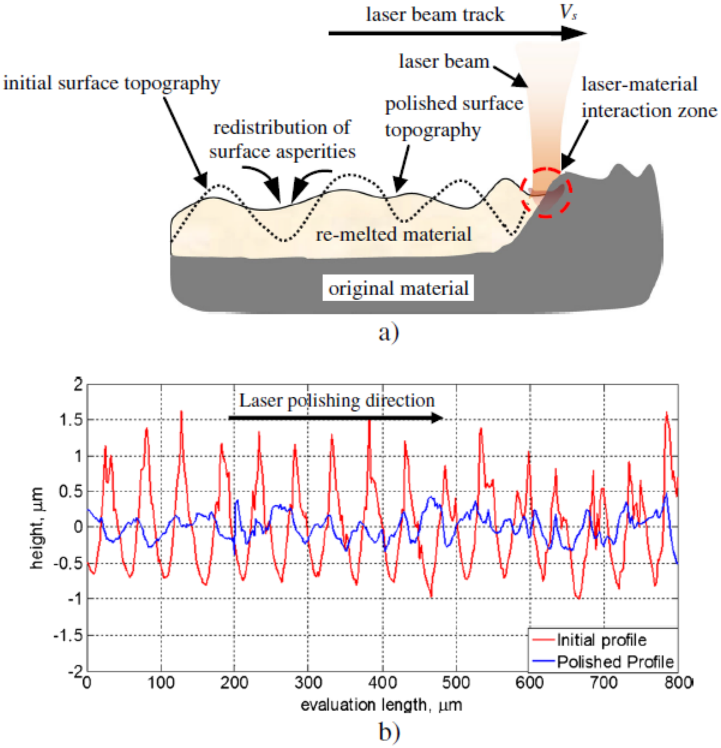
laser beam track
V_s
laser beam
initial surface topography
polished surface topography
laser-material interaction zone
redistribution of surface asperities
re-melted material
original material
a)
Laser polishing direction
height, μm
2
1.5
1
0.5
0
-0.5
-1
-1.5
-2
0
100
200
300
400
500
600
700
800
evaluation length, μm
Initial profile
Polished Profile
b)

Figure 2.7- Overview of laser polishing: a) Schematic of remelting mechanism, b) the effect of laser on surface micro-asperities (Bordatchev et al., 2014).

Surface finish always has been one of design and quality requirement for engineering parts. A number of researchers have identified two different operating regimes for the laser polishing process based on the energy density applied: shallow surface melting (SSM) and surface over melt (SOM). In the SSM regime, the thickness of the melted layer is less than the peak-to-valley height of the micro-milled track. Consequently, the molten material will naturally flow from the local maximum to the valleys under capillary pressure, and hence decrease the Ra over the heat affected region. If the thickness of the melted layer created by the laser beam is greater than the peak-to-valley height, then the original surface topology may disappear and a molten material pool can be created. Generally surface roughness is strongly correlated with three interdependent indicators including:

(1) Topographic quality and accuracy, precision and surface macro/micro asperities

(2) Functionality and tribological, optical and other physical-mechanical properties

(3) Esthetic and visual appearance

The surface roughness of a part or a product strongly influences its properties and functions. Among these can be counted: abrasion and corrosion resistance, tribological properties, optical properties, haptics as well as the visual impression the customer desires. Therefore, in industrial manufacturing, grinding and polishing techniques are widely used to reduce the roughness of surfaces. A point of interest is that laser polishing can improve these indicators altogether. It is worth to note here that conventional polishing methods (manual, mechanical and chemical) carried out in consecutive stages and almost always need inter-stage cleaning and, therefore it remarkably increases time, cost, and consequently reduce productivity of the whole process. By contrast, laser polishing systems configuration and control parameters system are more or less similar to a SLM machine since both process have laser energy source. Therefore, the time and efforts involved in laser polishing can be significantly reduced (Bordatchev et al., 2014).

2.10 Laser polishing (LP) and additive manufacturing (AM)

In this section, recent studies on laser polishing (LP) of AM processed parts especially selective laser melting process are presented. The idea of hybrid additive manufacturing (AM) and laser polishing (LP), can be set up with two different approchs. In the first approch, LP can be applied after each AM layer is created. The advantages of this approach is creation of 100% dense part and considerably decreased residul stress. This technique can be more time consuming but it is preferred for automotive, aerospace, and other fields of engineering where high mechanical strength and wear resistance are of paramount importance. The other approach is that LP only be applied after final (top) layer of AM. This approch can increase surface quality, however it has no positive effect on the reduction of part internal prosity, as only top layer is polished. Therefore, selection of the better approach has to be based on application and functionality of part component.

During last decade at least two comrehensive studies have been caried out on laser polishing of parts which were manufactured by SLM methods. Alrbaey et al. (2014) reported that for parts of 316L stainless steel manufactured by SLM with a initial surface roughness ranging from 8 μm to 20 μm, laser remelting caused an 80% decrease in surface roughness. It should be underscored here that they used DOE (Design of Experiment Method) for optimization of SLM and laser remelting separately. To circumvent limitation of Alrbaey's work, researchers such as Yasa et al. (2011) employed a comprehensive and systematic approach to investigate the joint effects of laser polishing process and SLM process that used a continuous wipe laser. Several papers are published based on this work, to report the outcomes for parts fabricated with commonly used metal powders such as 316L stainless steel and Ti-6Al-4V. This work have been referenced in almost all recent studies on laser polishing of metallic materials and alloys. It should be point out that similar systematic studies (Lamikiz et al., 2007) also have been conducted on SLS process and more or less similar results have been demonstrated.

Due to the nature of SLM which utilizes powder materials, in addition to surface roughness limitation, SLM also suffers from 1 to 2 percent of porosity. Polishing of the outer surface (after top layer) of SLM manufactured parts can only decrease surface porosity. For some critical applications, reduction of internal prosity certainly could expand its application in other industries. For this case, laser polishing after each layer melting in SLM is an effective but time consuming approach for improving parts quality.

It is concluded that, in the field of additive manufacturing, not enough work has been dedicated to laser re-melting, though laser surface modification of bulk materials has been studied extensively by some researchers as has been discussed in previous sections.

CHAPTER III

METHODOLOGY

In this chapter, all the experiments and utilized instrumentation are discussed. In the Materials and Methods sections, morphology and chemical properties of stainless steel powder are provided. In addition, technical specification of the additive manufacturing machine used for the experiments is described and details of file preparation with Magics® software are discussed. At the end of this chapter, tools which have been used for measuring design outcomes are discussed.

3.1 Materials

316L austenitic stainless steel powder was supplied by Renishaw plc. Chemical composition of powder is presented in table 3.1.

Table 3.1- Chemical composition (Weight %) of 316L stainless steel powder

Element	**Cr**	**Ni**	**Mo**	**Mn**	**Si**	**N**	**O**	**P**	**C**	**S**
Mass (%)	16 to 18	10 to 14	2 to 3	< 2	< 1	< 0.1	< 0.1	< 0.045	< 0.03	< 0.03

The particle size distribution of powder was 45+15 μm. Figure 3.1 shows the SEM of 316L austenitic stainless steel powder. As can be seen, the particles display a round shape morphology with an appropriate size distribution.

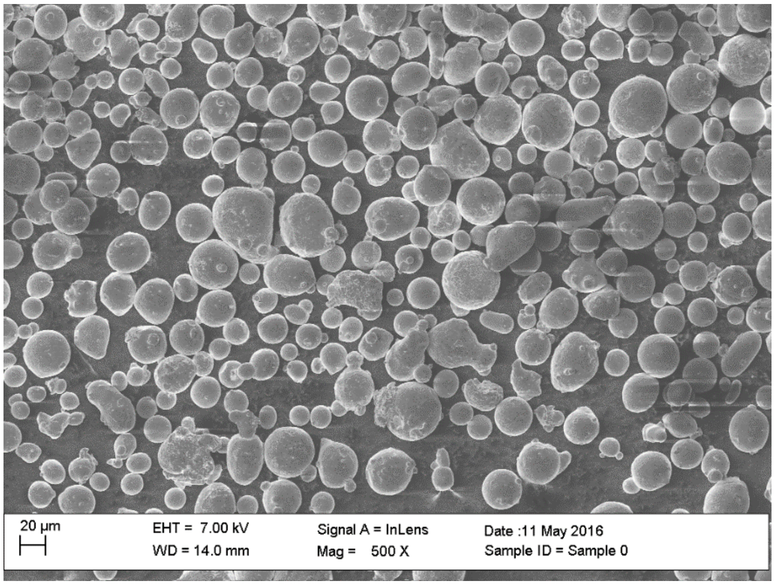
20 μm
EHT = 7.00 kV
WD = 14.0 mm
Signal A = InLens
Mag = 500 X
Date :11 May 2016
Sample ID = Sample 0

Figure 3.1- SEM image of 316L austenitic stainless steel powder

3.2 Selective Laser Melting System

A Renishaw AM 250 laser melting machine was used for preparing samples for this study. Figure 3.2 shows front view of this machine. Technical specifications of this machine are presented in Table 3.2.

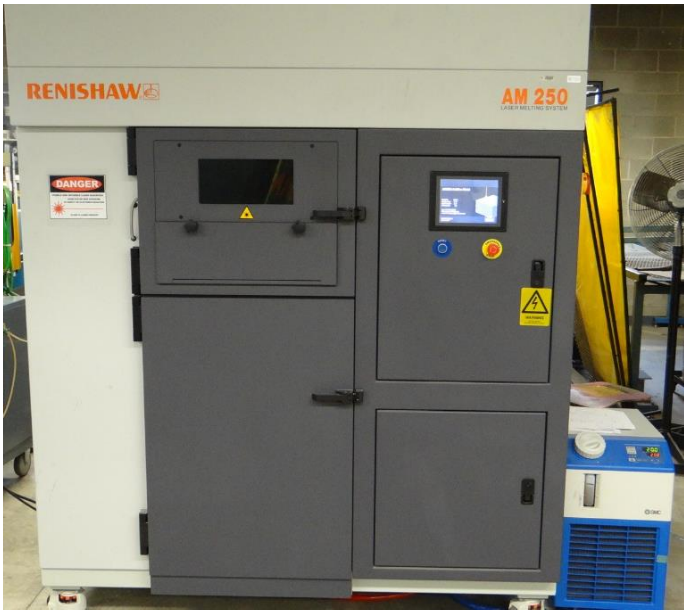

Figure 3.2- Renishaw AM 250 laser melting machine

Table 3.2-Technical specification of Renishaw AM 250 laser melting machine

Max part building area	245 x 245 x 300 mm (X, Y, Z)
Build rate	5 cm^3 - 20 cm^3 per hour
Scan Speed	Up to 2000 mm/s
Positioning speed(max)	7000 mm/s
Layer thickness	20 – 100 µm
Laser beam diameter	70 µm diameter at powder surface
Laser type	ytterbium fiber laser
Laser wavelength	1070 nm
Max laser power	200 Watt

3.3 Methods

Ultimate goal of this study is optimizing remelting process parameters. So, at first step, 4x4 test series (4 column and 4 rows) are printed in order to find a proper range of process parameters. It should be noted that at each test series, one input parameter varies in the row direction and another input parameter varies in the column direction, and all remaining process parameters remain constant. Figure 3.3 shows one of test series being used for finding appropriate range of vital parameters. Preliminary trial and error runs, machine technical specifications and also previously published works (Wang et al., 2016) were used for identifying the important input variables and the proper range for those input factors. At all examined levels of thickness of remelted shell, change of hatch distance reveals no effect on surface roughness. In other words, by fixing remelting layer thickness to 100 μm, 150 μm, or 200 μm, at each slice of remelting, laser swept the surface just one time and there is no overlap at each specific step. Four examined input variables are laser power, laser exposure time, point distance, and remelting layer thickness. It should be noted that for printing of base samples, layer thickness was fixed at 50 μm.

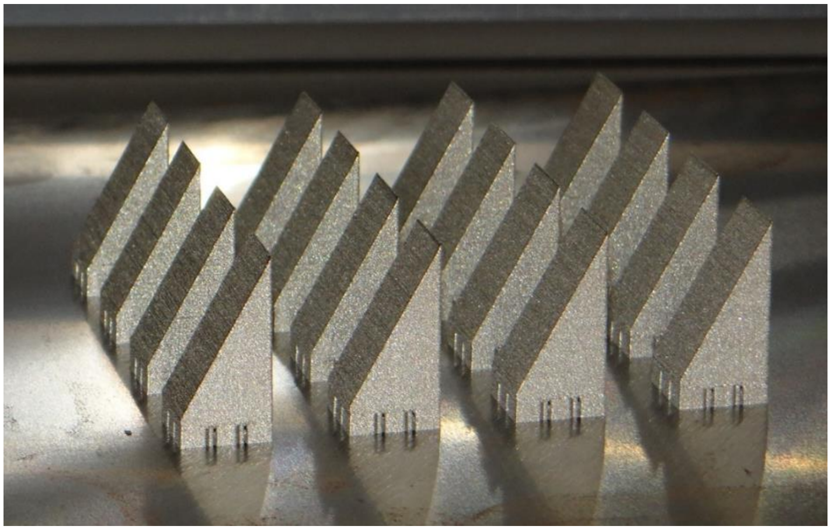

Figure 3.3- 4X4 printed test series

Based on primary trials and errors for finding the suitable range of process parameters, four vital process parameters (Table 3.3) were selected for laser remelting process. In this study, after having ranges for the four independent variables, Box-Behnken design of experiment is used for optimization. Based on the Box-Behnken design, totally twenty seven (27) experiments were carried out with four independent variables.

Table 3.3-Parameters and ranges for Box-Behnken design

Dependent Variables	**Coded and actual levels of dependent variables**		
	-1	**0**	**1**
A: Shell Layer Thickness, μm	100	150	200
B: Point Distance, μm	30	50	70
C: Laser Exposure Time , μs	200	300	400
D: Laser Power, Watt	150	175	200

Twenty seven pieces of 45^0 inclined samples were printed separately in order to meet randomization assumption of designed statistical study. It should be noted that all 27 samples were printed with the same process parameters in order to obtain the same initial surface roughness for all the samples. After completion of printing of each sample, the substrate was moved upward (to the initial position) and the powder around the sample was removed. At this step, laser remelting was conducted on the inclined surface of the sample. After completion of the remelting process, sample was removed from the substrate for evaluation of surface roughness. Figure 3.4 shows one of 27 samples after remelting and removal from the substrate.

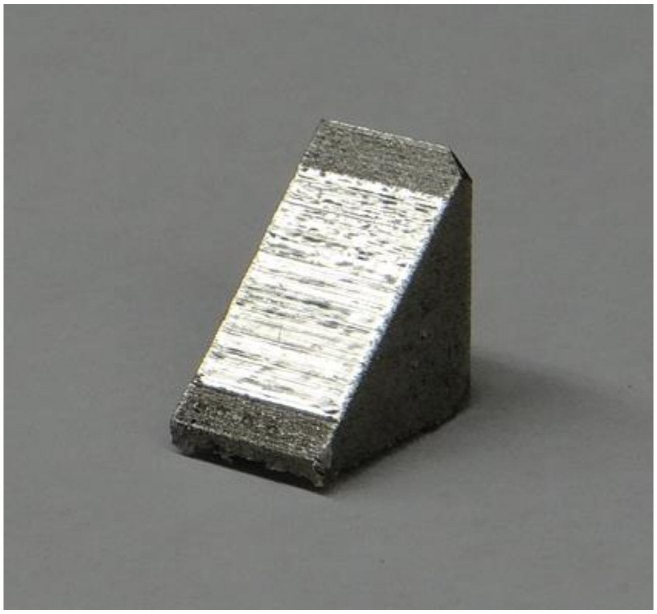

Figure 3.4- Typical SLM printed sample based on Box-Behnken design

3.3.1 CAD file preparation

Predefined slider type CAD model parts with the 45˚ slope were created using Materialize Magics® 19.02 3D Printing software. Figure 3.5 shows defined dimensions values for creating base sample (Figure 3.4) in Magics® software.

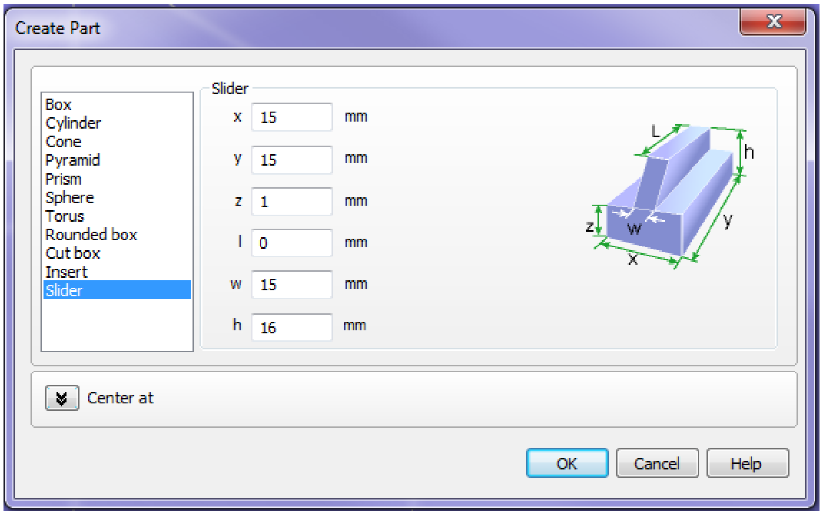
Create Part
Box
Cylinder
Cone
Pyramid
Prism
Sphere
Torus
Rounded box
Cut box
Insert
Slider
L
h
z
w
x
y
Center at
OK
Cancel
Help

Slider

x 15 mm

y 15 mm

z 1 mm

l 0 mm

w 15 mm

h 16 mm

Figure 3.5- Snapshot of creating 45 ° inclined sample file in Magics® software

Figure 3.6 shows the dimensions and orientation of the base sample in Magics® software along with supports for sample.

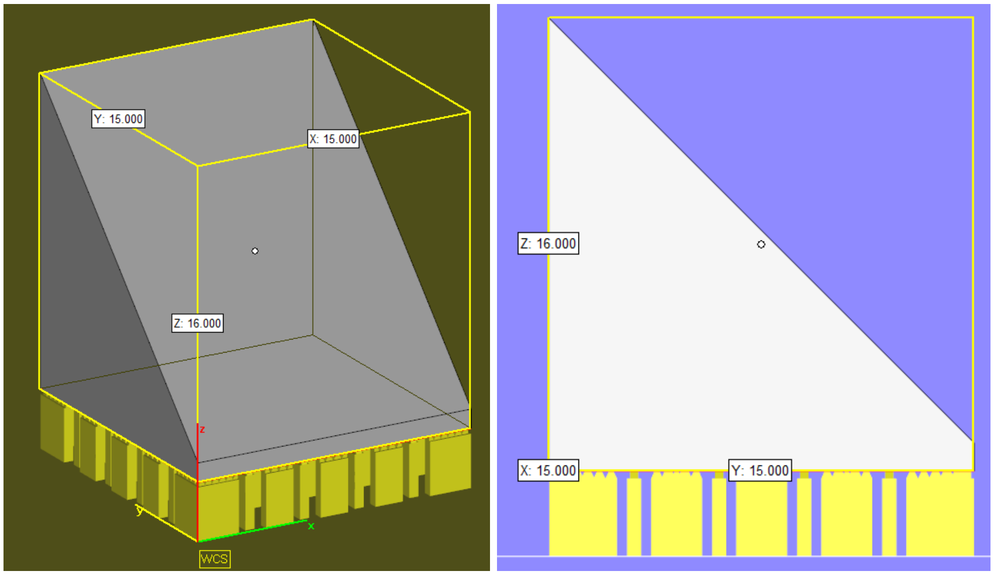
Y: 15.000
X: 15.000
Z: 16.000
z
y
x
WCS
Z: 16.000
X: 15.000
Y: 15.000

Figure 3.6- Dimensions and geometry of 45^0 inclined sample file along with support section in Magics® software

Predefined slider type CAD model parts with the 45^0 slope were created using Materialize Magics® 19.02 3D Printing software. Figure 3.7 shows method of creating remelting layer sample in Magics® software.

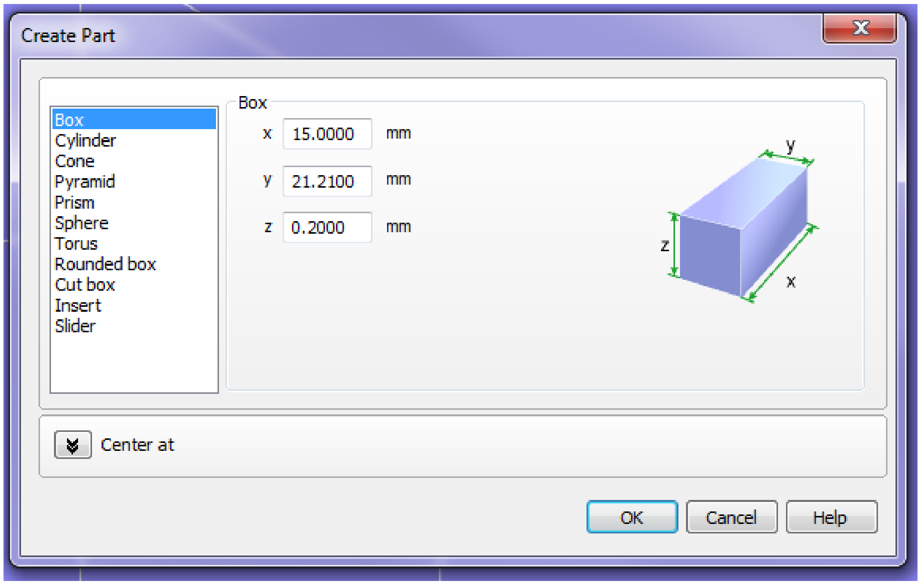

Create Part
Box
Cylinder
Cone
Pyramid
Prism
Sphere
Torus
Rounded box
Cut box
Insert
Slider
Box
y
z
x
Center at
OK
Cancel
Help

x 15.0000 mm

y 21.2100 mm

z 0.2000 mm

Figure 3.7- Snapshot of creating 45^0 inclined remelting layer file in Magics® software

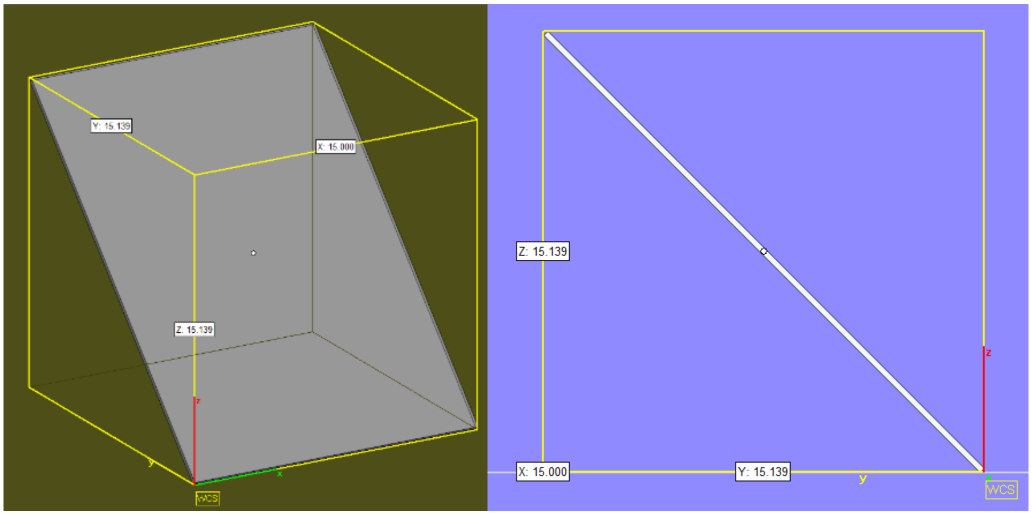

Figure 3.8- Dimensions and geometry of 45^0 inclined thin layer file in Magics® software

Due to the unique orientation of sample, nature of scan strategy for remelting process is very important. Figure 3.9 display scan strategy for remelting of inclined surface.

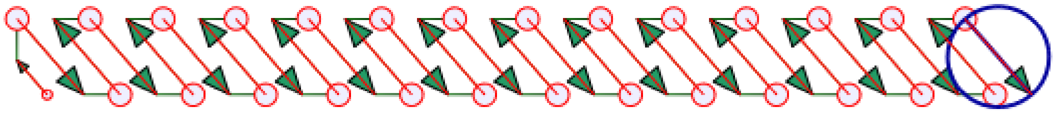

Figure 3.9- Scan strategy in Renishaw build processor slice viewer

Relationship between slice thickness and number of slices for three different slice thicknesses is presented in table 3.4. As this table illustrates, with increasing the slice thickness, number of slice will decrease.

Table 3.4- Relationship between slice thickness and number of slices

Slice Thickness	Shell Height	Number of shell slice (Layer)
100 µm	15.00 mm	151
150 µm	15.00 mm	101
200 µm	15.00 mm	76

The hatch scanning parameters for printing of base samples were fixed based on Renishaw build processer as follows: Power: 200 Watt, Exposure Time: 80 µs, Point Distance: 50 µm, Focus offset: 0 mm, Build Strategy type: Meander, Hatch Distance: 50 µm, Hatching Rotation Angle (Increment value) : 67^0. In addition, for shell printing build strategy was meander with focus as zero. Since measurement of roughness on inclined surface is impossible so all samples after printing and removing from substrate were mounted by Buehler manual metallurgical sample mounting press (Figure 3.10).

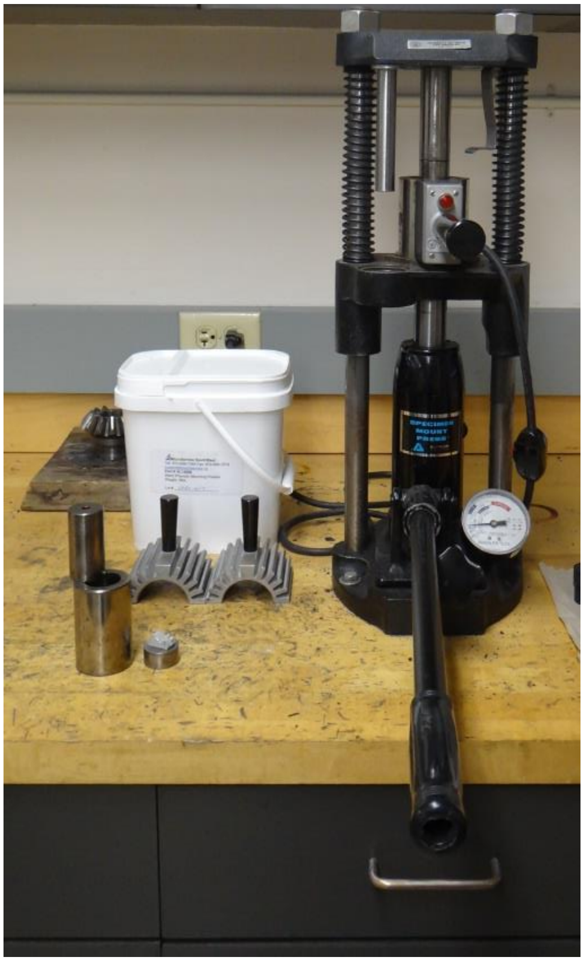

Figure 3.10- Manual metallurgical sample mounting press

Figure 3.11 displays some of printed samples in mounted condition.

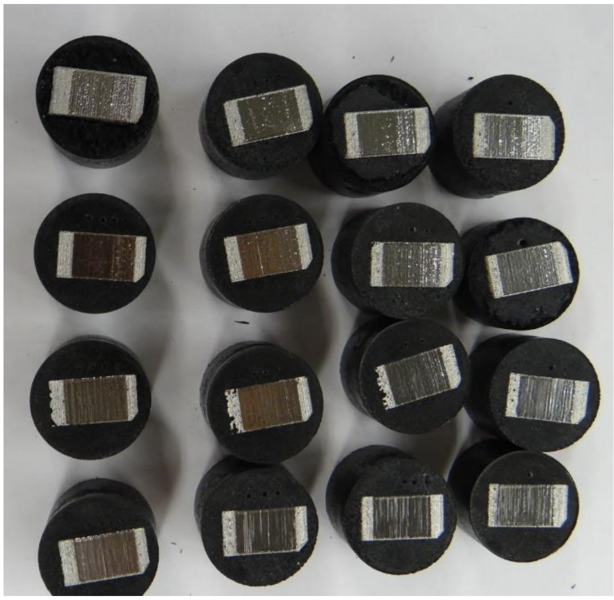

Figure 3.11- Some of samples after mounting process

3.4 Surface roughness evaluation

A Marsurf M300-C mobile roughness measuring instrument (figure 3.12) was used for measuring surface roughness of inclined samples after mounting. The roughness tester measures both the arithmetic mean surface roughness (Ra) and the surface roughness depth (Rz). Since both measurements show the same trend (for each measurement, value of Rz is around 4 times the value of Ra), in this study the roughness of the samples are reported only by the arithmetic mean surface roughness (Ra). An example of roughness measurement on non-remelted (initial) surface and an example of roughness measurement on remelted (final) surface are presented in figures 3.13 and 3.14 respectively.

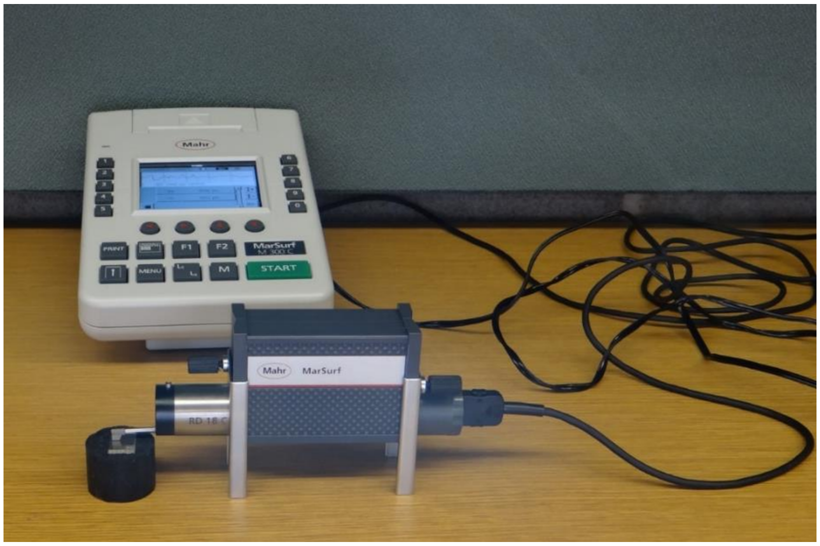
Mahr
PRINT
F1
F2
MarSurf
M 300 C
MENU
M
START
Mahr MarSurf

Figure 3.12- roughness measuring instrument set up

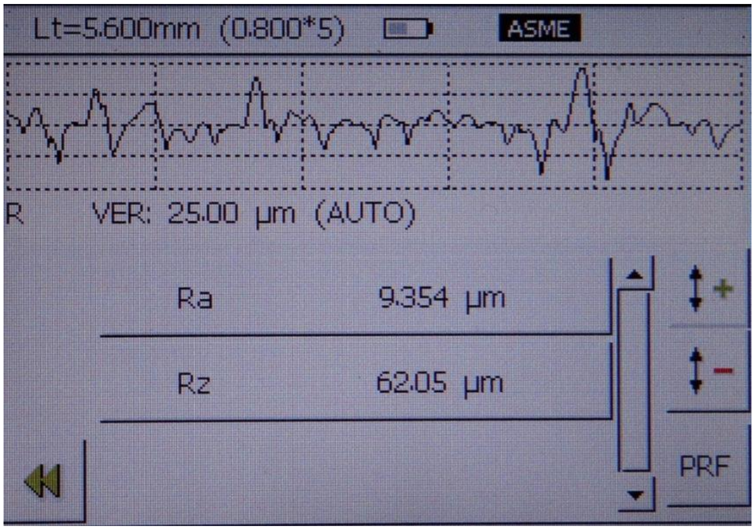
Lt=5.600mm (0.800*5)

ASME

R VER: 25.00 µm (AUTO)

Ra 9.354 µm

Rz 62.05 µm

Figure 3.13- A sample of roughness measurement on not remelted (initial) surface

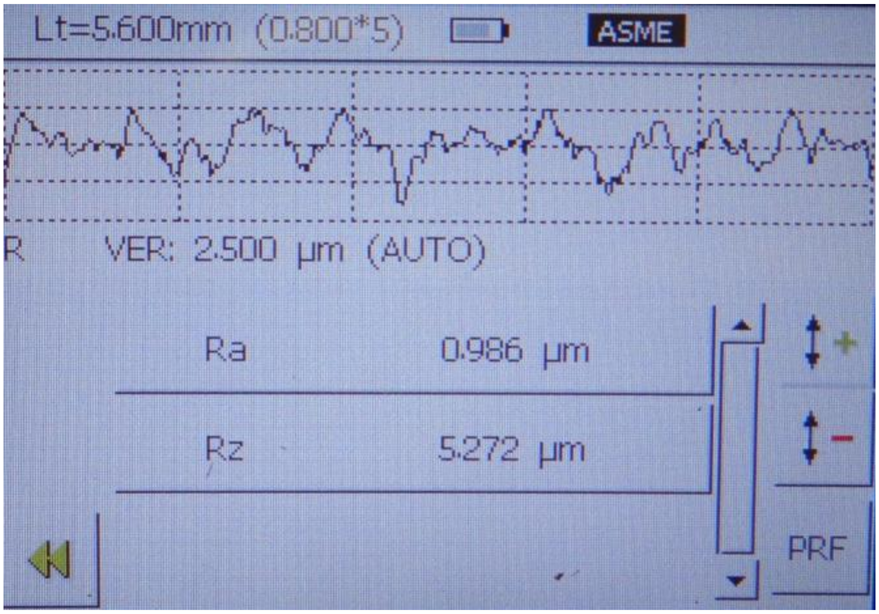

Lt=5.600mm (0.800*5)

VER: 2.500 µm (AUTO)

Ra 0.986 µm

Rz 5.272 µm

Figure 3.14- A sample of roughness measurement on remelted (final) surface

The morphology and surface of samples after remelting were investigated via a Carl Zeiss Sigma VP scanning electron microscope.

ZEISS
EDAX
EDAX
Periodic Table of Elements

Figure 3.15- scanning electron microscope set up

CHAPTER IV

RESULTS AND DISCUSSION

This chapter starts with a brief explanation of design of experiment. Then the Box-Behnken design method of Response Surface Methodology (RSM) is discussed. Response Surface Methodology (RSM) was introduced by Box and Wilson. Main process parameters and results of this study based on this DoE tool are summarized in separate tables. The main effect and interaction plot of the experiment are displayed and discussed in detail. ANOVA analysis is used repeatedly in this chapter in order to fit the regression models to be developed. Assumptions of ANOVA and regression were validated by the study of residual plots and probability plots. At the end of this chapter, contour plots and surface plots are represented for visualization of results. Finally optimization conditions for response variable (surface roughness) are discussed.

4.1 Experimental design and modeling

Design of experiment (DoE) means finding any cause-and-effect relationships in a process, product or system by purposefully changing the input parameters and then measuring the desired output factors. Ultimately, DoE enables researchers to develop a mathematical and/or empirical model to relate the system output variables to the system input variables and therefore facilitate system improvement and/or decision making on the system. RSM is among the main categories of DoE techniques. In fact, it is one of the mathematical or statistical modeling tools.

RSM is widely used in industry and academia to study relationship between independent and dependent variables of any interested process or system. Most of the time, the approach is that a few key independent and controllable variables under investigation system are first identified. At next step, RSM tools are utilized to find appropriate level of input factors that optimize the response variables. Whenever there is doubt about the curvature in response surface, RSM is an acceptable choice. Box-Behnken designs and central composite designs are the most popular RSM statistical tools. It should be noted that there are five experimental levels for the central composite approach but a Box-Behnken design is a three level experimental design. Design points are located either at the center of design or at the center of each edge of the cube.

In fact, the design points are never chosen at low or high levels for all variables concurrently. Possibility of efficient prediction of quadratic polynomial terms in a regression equation, fewer number of runs in comparison to central composite design, and all points being within safe variables range, are fundamental characteristics of Box-Behnken design (C. Montgomery, 2012). Box–Behnken design of experiments matrix and results are displayed in Table 4.1. This table includes input variables in both coded and actual conditions. Based on this table the minimum measured value for the response variable is 0.91 μm and the maximum measured response variable is 7.19 μm.

Table 4.1- Box–Behnken design of experiments matrix and results

Run Order	**Coded (Dimensionless) Input Variables**				**Actual Input Variables**				**Response Variable**	
	T	D	E	P	Remelting Layer Thickness (µm)	Point Distance (µm)	Laser Exposure Time (µs)	Laser Power (Watt)	Measured Roughness (Ra(µm))	Calculated Roughness (Ra(µm))
1	0	0	+1	-1	150	50	400	150	0.76	0.91
2	-1	0	0	-1	100	50	300	150	3.43	3.68
3	-1	0	0	+1	100	50	300	200	2.45	2.22
4	0	0	-1	-1	150	50	200	150	6.00	5.97
5	0	0	0	0	150	50	300	175	1.85	1.85
6	0	+1	+1	0	150	70	400	175	2.27	1.98
7	0	0	+1	+1	150	50	400	200	1.45	1.46
8	-1	-1	0	0	100	30	300	175	3.84	3.73
9	+1	0	+1	0	200	50	400	175	2.20	2.29
10	0	0	-1	+1	150	50	200	200	4.68	4.70
11	0	+1	0	-1	150	70	300	150	3.22	3.02
12	0	+1	-1	0	150	70	200	175	4.83	4.60
13	0	-1	0	+1	150	30	300	200	3.60	3.72
14	0	-1	0	-1	150	30	300	150	4.60	4.28
15	0	-1	-1	0	150	30	200	175	6.83	7.19
16	+1	0	-1	0	200	50	200	175	6.21	6.24
17	0	+1	0	+1	150	70	300	200	2.62	2.85
18	-1	0	-1	0	100	50	200	175	5.65	5.47
19	0	0	0	0	150	50	300	175	1.65	1.85
20	0	0	0	0	150	50	300	175	2.06	1.85

21	+1	+1	0	0	200	70	300	175	3.54	3.63
22	-1	+1	0	0	100	70	300	175	2.92	3.29
23	+1	0	0	-1	200	50	300	150	3.24	3.55
24	+1	-1	0	0	200	30	300	175	5.71	5.32
25	0	-1	+1	0	150	30	400	175	1.20	1.51
26	-1	0	+1	0	100	50	400	175	1.25	1.13
27	+1	0	0	+1	200	50	300	200	4.45	4.28

4.2 Main effects of process independent variables on surface roughness

Based on the data from the Box–Behnken design of experiments matrix and results (Table 4.1), the main effects plot are presented in Figure 4.1 Main effect plot is a subcategory of factorial plot and displays the effect of input variable level on the mean of the response variable.

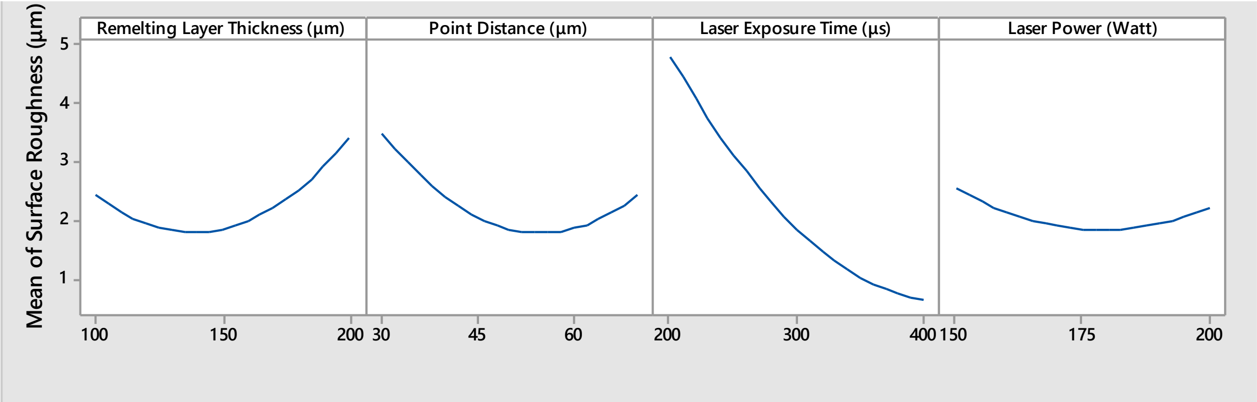

Figure 4.1- Main effects plot for response (fitted means)

MINITAB® software was used to calculate magnitudes of the main effects of the four involved independent variables (remelting layer thickness, point distance, laser exposure time, and laser power) on surface roughness as dependent variable of this study. Outcomes of calculation are presented in Figure 4.1.

4.2.1 Effect of remelting layer thickness

Considering remelting layer thickness, it is demonstrated that this parameter has a remarkable effect on study response. For the range of study, at lower layer thickness, mean effect of this factor is about 2.5 µm. Then, with the increase of layer thickness, mean effect decreases to around 1.6 µm, however with increase of layer thickness beyond 150 µm, main effect increase considerably. During preliminary study for choosing appropriate range for input variables, a sample with minimum possible layer thickness by software (10 µm) and a sample with extraordinarily high layer thickness (500 µm) remelted. It was observed that when layer thickness is 10 µm, Ra rapidly increases to above 5 µm. This detrimental effect possibly is attributed to the high input of energy that causes dimensional inaccuracy and surface deflection. Lower remelting layer thickness decreases the production rate as well. Therefore, remelting layer thickness below 100 µm is not efficient and effective at all. On the other hand, for remelting layer thickness 500 µm, it was noticed that remelting was not able to cover all the surface. Therefore consecutive remelted and un-remelted bands again resulted with surface inhomogeneity and increase of surface roughness (Li et al., 2009).

4.2.2 Point distance effect

As Figure 4.1 displays, at lower range of point distance, mean effect of this parameter on response variable is close to 3 μm but with increase of point distance, first this effect moderately decreases and reaches a value around 50 μm and after that increase of point distance results in gradually increase of surface roughness.

4.2.3 Laser exposure time effect

The graphs showing main effects indicate that laser exposure time has the highest effect on surface roughness among four studied factors. At 200 μs of exposure, mean of surface roughness is close to 5 μm. With increase of exposure time, the mean of surface roughness dramatically deceases. At the upper extreme of laser exposure time range slowly heat a low point of 0.5 μm mean effect.

4.2.4 Laser power effect

The graphs showing main effects indicate that laser power has the least effect on surface roughness among four studied factors. At 150 watt of laser power, the mean of surface roughness is near 2 μm and slowly decreases with increase of laser power and then reaches its lower point around 180 watt. From 180 watt to 200 watt, mean of surface roughness shows a gradually upward trend. In other words, across all laser power levels, the response mean stays approximately at the same level.

4.3 Interaction plots for response

Figure 4.2 is interaction plot for the variables. In general, interaction occurs whenever influence of one input variable is influenced by the level of another input variable. Figure 4.2 shows that effect of laser power is dependent on level of layer thickness, effect of laser exposure time is dependent on point distance, effects of both point distance and laser power are dependent on level of laser exposure time, and both layer thickness and laser exposure time are dependent on laser power (Lavvafi, 2013). It should be noted that laser exposure time has highest amount of effect on point distance and laser power.

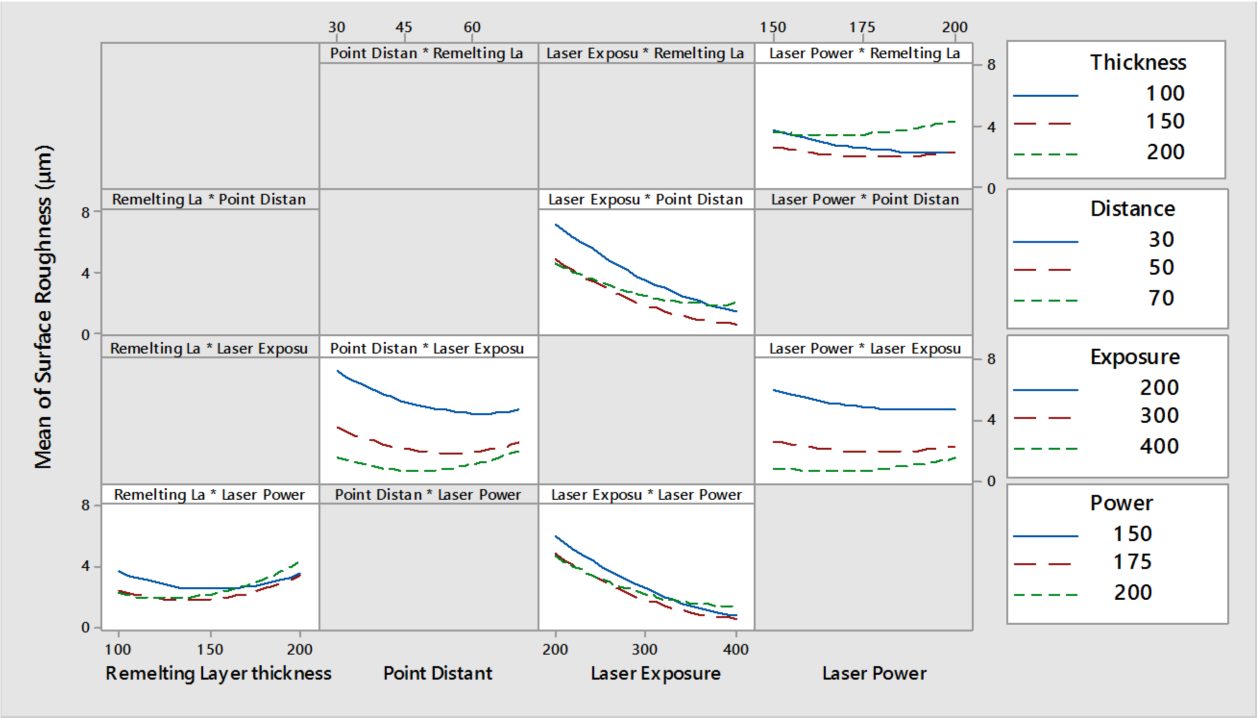

Figure 4.2- Interaction plots for response (fitted means)

4.4 Analysis of variance (ANOVA) and effect of input parameters

The reality is that the main effects are not able to illustrate interaction among experiment independent variables and nature of their impacts on the surface roughness. Therefore, the RSM tool was utilized to examine the cross effects. In order to fit a regression model to response surface design, Box–Behnken design of experiments matrix and results were analyzed by use of Minitab surface response design analyzer. At initial step, full quadratic terms (linear, squares, and interactions) were included for fitting in analyzer.

The general approach for modeling of independent process variable is that first fitness of a first-order regression model is examined. In case the first order model reveals remarkable lack of fit then the second order model is examined. Analysis of variance for first order model indicates considerable lack of fit (i.e. P-Value =0.05 for Lack-of-Fit, R^2, R^2 adjusted, R^2 predicted respectively are 78.24%, 74.29%, and 70.65%). Therefore, at this step it can be concluded that range of initial parameters is not in remote are of response surface and set of values are suitable for approaching to valley of response surface. In other words, second order model will be a better fit for these experiments.

For second order modeling analysis of variance, model summary, and coded coefficients are outcomes of analyzer (Minitab® software) which are presented in Table 4.2 through Table 4.8. In this study, in analysis of variance table, P-value approach is being used for testing the hypothesis and will fail to reject H0 if statistic F0 is more than predefined alpha value. Results of ANOVA analysis for surface roughness are presented in Table 4.2. As this table illustrates, P-values of linear terms of T, D, and E, all square terms (T*T, D*D, E*E, P*P), and two way interaction terms of T*P, D*E, E*P statistically are significant and play a role in the response (surface roughness) regression equation. As Table 4.2 shows, value of lack-of-fit for this analysis is 0.254. This non-significant value implies that relevant surface roughness regression model could properly define the relationship between four input variables (remelting layer thickness, point distance, laser exposure time, and laser power) and response variable (surface roughness). In ANOVA table R^2 as coefficient of multiple determinations is defined by the following equation:

$$R^2 = \frac{SS_R}{SS_T} = 1 - \frac{SS_E}{SS_T}$$

Where SS_T is total sum of squares, SS_R is sum of squares due to the regression and SS_E sum of squares due to residual error. Since R^2 value always increases with adding terms to the regression model, the adjusted R^2 statistic which is defined by the following equation is more applicable.

$$R^2_{\text{adj}} = 1 - \frac{SS_E/(n-p)}{SS_T/(n-1)} = 1 - \left(\frac{n-1}{n-p}\right)(1 - R^2)$$

In general, if an inappropriate term is added, the value of R^2 adjusted will almost always increase.

Table 4.2-Analysis of Variance for surface roughness including all quadratic terms

Source	DF	Adj SS	Adj MS	F-Value	P-Value
Model	14	74.0732	5.2909	49.90	0.000
Linear	4	58.9522	14.7381	138.99	0.000
T	1	2.8130	2.8130	26.53	0.000
D	1	3.3920	3.3920	31.99	0.000
E	1	52.4172	52.4172	494.33	0.000
P	1	0.3300	0.3300	3.11	0.103
Square	4	10.0770	2.5192	23.76	0.000
T*T	1	6.0161	6.0161	56.74	0.000
D*D	1	6.4338	6.4338	60.68	0.000

```
    E*E                1   3.9982   3.9982    37.71    0.000
    P*P                1   1.3986   1.3986    13.19    0.003
  2-Way Interaction    6   5.0440   0.8407     7.93    0.001
    T*D                1   0.3906   0.3906     3.68    0.079
    T*E                1   0.0380   0.0380     0.36    0.560
    T*P                1   1.1990   1.1990    11.31    0.006
    D*E                1   2.3562   2.3562    22.22    0.001
    D*P                1   0.0400   0.0400     0.38    0.551
    E*P                1   1.0201   1.0201     9.62    0.009
Error                 12   1.2724   0.1060
  Lack-of-Fit         10   1.1884   0.1188     2.83    0.289
  Pure Error           2   0.0841   0.0420
Total                 26  75.3457
Model Summary
       S    R-sq  R-sq(adj)  R-sq(pred)
0.325633  98.31%     96.34%      90.66%
```

Table 4.3-Estimated Coded Coefficients for surface response including all quadratic terms

```
Term        Effect      Coef  SE Coef  T-Value  P-Value   VIF
Constant               1.853    0.188     9.86    0.000
T           0.9683    0.4842   0.0940     5.15    0.000  1.00
D          -1.0633   -0.5317   0.0940    -5.66    0.000  1.00
E          -4.1800   -2.0900   0.0940   -22.23    0.000  1.00
P          -0.3317   -0.1658   0.0940    -1.76    0.103  1.00
T*T          2.124     1.062    0.141     7.53    0.000  1.25
D*D          2.197     1.098    0.141     7.79    0.000  1.25
E*E          1.732     0.866    0.141     6.14    0.000  1.25
```

P*P	1.024	0.512	0.141	3.63	0.003	1.25
T*D	-0.625	-0.312	0.163	-1.92	0.079	1.00
T*E	0.195	0.098	0.163	0.60	0.560	1.00
T*P	1.095	0.547	0.163	3.36	0.006	1.00
D*E	1.535	0.768	0.163	4.71	0.001	1.00
D*P	0.200	0.100	0.163	0.61	0.551	1.00
E*P	1.010	0.505	0.163	3.10	0.009	1.00

Considering P-Values in both analysis of variance table and coded coefficient tables, it is evident that three of two-way interaction terms have non-significant P-Values including T*D, T*E, and D*P. Since the two-way interaction term T*E has the highest P-Value, term will be removed from quadratic equation at this step. It should be noted that at this step R squared values and lack-of-fit values seems reasonable. The refitted model after removing term T*E is presented in Table 4.4.

Table 4.4- Analysis of Variance for surface roughness after removing term T*E

Source	DF	Adj SS	Adj MS	F-Value	P-Value
Model	13	74.0352	5.6950	56.50	0.000
Linear	4	58.9523	14.7381	146.20	0.000
T	1	2.8130	2.8130	27.91	0.000
D	1	3.3920	3.3920	33.65	0.000
E	1	52.4172	52.4172	519.99	0.000
P	1	0.3300	0.3300	3.27	0.094
Square	4	10.0770	2.5192	24.99	0.000
T*T	1	6.0161	6.0161	59.68	0.000

D*D	1	6.4338	6.4338	63.82	0.000
E*E	1	3.9982	3.9982	39.66	0.000
P*P	1	1.3986	1.3986	13.87	0.003
2-Way Interaction	5	5.0060	1.0012	9.93	0.000
T*D	1	0.3906	0.3906	3.88	0.071
T*P	1	1.1990	1.1990	11.89	0.004
D*E	1	2.3562	2.3562	23.37	0.000
D*P	1	0.0400	0.0400	0.40	0.540
E*P	1	1.0201	1.0201	10.12	0.007
Error	13	1.3105	0.1008		
Lack-of-Fit	11	1.2264	0.1115	2.65	0.306
Pure Error	2	0.0841	0.0420		
Total	26	75.3457			
Model Summary					
S	R-sq	R-sq(adj)	R-sq(pred)		
0.317498	98.26%	96.52%	90.81%		

Table 4.5-Estimated Coded Coefficients for surface roughness after removing term T*E

Term	Effect	Coef	SE Coef	T-Value	P-Value	VIF
Constant		1.853	0.183	10.11	0.000	
T	0.9683	0.4842	0.0917	5.28	0.000	1.00
D	-1.0633	-0.5317	0.0917	-5.80	0.000	1.00
E	-4.1800	-2.0900	0.0917	-22.80	0.000	1.00
P	-0.3317	-0.1658	0.0917	-1.81	0.094	1.00
T*T	2.124	1.062	0.137	7.73	0.000	1.25
D*D	2.197	1.098	0.137	7.99	0.000	1.25
E*E	1.732	0.866	0.137	6.30	0.000	1.25

P*P	1.024	0.512	0.137	3.72	0.003	1.25
T*D	-0.625	-0.312	0.159	-1.97	0.071	1.00
T*P	1.095	0.548	0.159	3.45	0.004	1.00
D*E	1.535	0.768	0.159	4.83	0.000	1.00
D*P	0.200	0.100	0.159	0.63	0.540	1.00
E*P	1.010	0.505	0.159	3.18	0.007	1.00

At this stage, still two-way interaction terms of T*D and D*P have non-significant (>0.05) values of P-Values. R squared values and lack-of-fit values seem reasonable. Since term D*P has the higher non-significant P-Value, it was removed from regression equation terms. The refitted model after removing term D*P is presented in Table 4.6.

Table 4.6-Analysis of Variance for surface roughness after removing term D*P

Source	DF	Adj SS	Adj MS	F-Value	P-Value
Model	12	73.9952	6.1663	63.92	0.000
Linear	4	58.9522	14.7381	152.79	0.000
T	1	2.8130	2.8130	29.16	0.000
D	1	3.3920	3.3920	35.16	0.000
E	1	52.4172	52.4172	543.40	0.000
P	1	0.3300	0.3300	3.42	0.086
Square	4	10.0770	2.5192	26.12	0.000
T*T	1	6.0161	6.0161	62.37	0.000
D*D	1	6.4338	6.4338	66.70	0.000
E*E	1	3.9982	3.9982	41.45	0.000
P*P	1	1.3986	1.3986	14.50	0.002

2-Way Interaction	4	4.9660	1.2415	12.87	0.000
T*D	1	0.3906	0.3906	4.05	0.064
T*P	1	1.1990	1.1990	12.43	0.003
D*E	1	2.3562	2.3562	24.43	0.000
E*P	1	1.0201	1.0201	10.58	0.006
Error	14	1.3505	0.0965		
Lack-of-Fit	12	1.2664	0.1055	2.51	0.320
Pure Error	2	0.0841	0.0420		
Total	26	75.3457			

Model Summary

S	R-sq	R-sq(adj)	R-sq(pred)
0.310583	98.21%	96.67%	91.81%

Table 4.7-Estimated Coded Coefficients for surface roughness after removing term D*P

Term	Effect	Coef	SE Coef	T-Value	P-Value	VIF
Constant		1.853	0.179	10.34	0.000	
T	0.9683	0.4842	0.0897	5.40	0.000	1.00
D	-1.0633	-0.5317	0.0897	-5.93	0.000	1.00
E	-4.1800	-2.0900	0.0897	-23.31	0.000	1.00
P	-0.3317	-0.1658	0.0897	-1.85	0.086	1.00
T*T	2.124	1.062	0.134	7.90	0.000	1.25
D*D	2.197	1.098	0.134	8.17	0.000	1.25
E*E	1.732	0.866	0.134	6.44	0.000	1.25
P*P	1.024	0.512	0.134	3.81	0.002	1.25
T*D	-0.625	-0.312	0.155	-2.01	0.064	1.00
T*P	1.095	0.548	0.155	3.53	0.003	1.00
D*E	1.535	0.768	0.155	4.94	0.000	1.00

E*P	1.010	0.505	0.155	3.25	0.006	1.00

At this stage, the two-way interaction term of T*D still has a non-significant (0.064>0.05) P-Value. R squared values and lack-of-fit values seem reasonable. At this step, term T*D was removed from regression equation terms. The refitted model after removing term T*D is presented in Table 4.8. Analysis of Variance for surface roughness after removing term T*D and estimated coded coefficients for surface roughness after removing term T*D were shown in Table 4.8.

Table 4.8-Analysis of Variance for surface roughness after removing term T*D

Source	DF	Adj SS	Adj MS	F-Value	P-Value
Model	11	73.6046	6.6913	57.65	0.000
Linear	4	58.9522	14.7381	126.97	0.000
T	1	2.8130	2.8130	24.23	0.000
D	1	3.3920	3.3920	29.22	0.000
E	1	52.4172	52.4172	451.59	0.000
P	1	0.3300	0.3300	2.84	0.112
Square	4	10.0770	2.5192	21.70	0.000
T*T	1	6.0161	6.0161	51.83	0.000
D*D	1	6.4338	6.4338	55.43	0.000
E*E	1	3.9982	3.9982	34.45	0.000
P*P	1	1.3986	1.3986	12.05	0.003
2-Way Interaction	3	4.5754	1.5251	13.14	0.000
T*P	1	1.1990	1.1990	10.33	0.006
D*E	1	2.3562	2.3562	20.30	0.000
E*P	1	1.0201	1.0201	8.79	0.010

```
Error               15   1.7411   0.1161
  Lack-of-Fit       13   1.6570   0.1275     3.03    0.275
  Pure Error         2   0.0841   0.0420
Total               26  75.3457
Model Summary
       S    R-sq  R-sq(adj)  R-sq(pred)
0.340695  97.69%     95.99%      92.08%
```

At this stage, all remaining terms of regression model have significant P-values apart from linear term D (P-Value as 0.112). Having removed all non-significant terms, the following revised regression models (both coded and uncoded) were obtained. In the final model, P-Value for lack-of-fit is 0.275 which is not statistically significant. Therefore, final model does not reveal any lack-of-fit. Additionally, bottom of ANOVA tables also summarize values of regression model such as R^2, R^2 adjusted, and R^2 predicted. Values for these statistical parameters could vary between 0 and 100%. In general, higher values of these parameters are desirable. As Table 4.8 shows, R^2 value is 97.69%. R^2 also is known as the determination coefficient. For the purpose of this study, it means that 97.69% of the variability in surface roughness can be explained by the final proposed regression model. R^2 adjusted value is 95.99%. Typically, adding a new term in the regression model results in increase of R^2, however this does not necessarily imply that newly added term improves the fitness of regression model (Wu et al., 2009).

Therefore, R^2 adjusted is a better indicator to check whether adding a new term to the regression model increase its fit or not. As discussed previously, one of the main objectives of DoE and the proposed regression model is to predict effects of future sets of input variables on the response variable. In other words, R^2, and R^2 adjusted are good indicators for examining the current status of the model but R^2 predicted is used for accuracy of the model for future observations of the system or process. The R^2 predicted value is 92.08%.

4.5 Transformation necessity

In addition to ANOVA, Box-Cox transformation procedure was applied on experimental data in order to check whether there is room for improving normality and equality of variance over variable ranges. Indeed, major violations of normality and equality assumptions increase the likelihood of type I or type II errors (Hamze et al, 2015). Calculated values of rounded λ and estimated λ are 1 and 0.96831, repeatedly. In addition, with 95% confidence interval, the value of λ is located between 0.611810 and 1.33681. The value of rounded λ implies that no transformation is required and utilizing Box-Cox transformation only makes available results identical to before transformation.

4.6 Fitting Regression Model

In many of engineering and scientific systems, each dependent variable is related to several input variables. Thus, developing a reliable mathematical or regression model to appropriately display the functional relationship between regression variables and output variables is very useful since the model can be easily utilized for several purposes including process control, optimization of process, and future status prediction. Often the cause and effect relationship between dependent and independent variables is not perfect. Therefore, first and second order polynomial regression models are used in order to approximate functional relationship. Design of experiments methods highly rely on regression for quantitative modeling and analyzing the data (Montgomery et al., 2006).

Table 4.9-Estimated Coded Coefficients for surface roughness after removing term T*D

Term	Effect	Coef	SE Coef	T-Value	P-Value	VIF
Constant		1.853	0.197	9.42	0.000	
T	0.9683	0.4842	0.0984	4.92	0.000	1.00
D	-1.0633	-0.5317	0.0984	-5.41	0.000	1.00
E	-4.1800	-2.0900	0.0984	-21.25	0.000	1.00
P	-0.3317	-0.1658	0.0984	-1.69	0.112	1.00
T*T	2.124	1.062	0.148	7.20	0.000	1.25
D*D	2.197	1.098	0.148	7.45	0.000	1.25
E*E	1.732	0.866	0.148	5.87	0.000	1.25
P*P	1.024	0.512	0.148	3.47	0.003	1.25
T*P	1.095	0.547	0.170	3.21	0.006	1.00
D*E	1.535	0.768	0.170	4.51	0.000	1.00
E*P	1.010	0.505	0.170	2.96	0.010	1.00

4.6.1 Regression Equation in Uncoded (actual) Units

Developing a suitable regression model for predicting the relationship among input and outputs of a process is one of the main objectives of statistical DoE analysis. For this study, regression equation in uncoded units for this set of experiment is as follows:

Surface roughness (µm) = 86.3 - 0.1944 T - 0.4163 D - 0.1274 E - 0.4197 P + 0.000425 T*T + 0.002746 D*D + 0.000087 E*E + 0.000819 P*P + 0.000438 T*P + 0.000384 D*E + 0.000202 E*P

4.6.2 Regression Equation in coded (dimensionless) Units

Regression analysis is a statistical modeling approach that is widely used to estimate the relationships among system input and output variables. The ranges of values for the coded variables are -1.0 to1.0. Regression equation in coded units for this experiment is as follows:

Surface roughness (µm) = 1.853 +0.4842 T - 0.5317 D – 2.09 E - 0.1658 P + 1.062 T*T + 1.098 D*D + 0.866 E*E + 0.512 P*P + 0.547 T*P + 0.768 D*E + 0.505 E*P

4.7 Validate model assumptions in regression or ANOVA

ANOVA analysis was used for statistical analysis of results of this study. Similar to a variety of statistical techniques, in ANOVA analysis also some assumptions should be carefully considered for robust and reliable application of analysis. The first assumption is that the residual of both independent and dependent variables should have normal distribution. Homoscedasticity or homogeneity of variance is the second assumption that should be fulfilled. From latter assumption constant variance or close to constant variance of a variable over the space of analysis of variable is expected. Due to importance of these two underlying assumptions, at this very beginning step, normality of residuals versus both four input parameters and the surface roughness output parameter was examined (Osborne, 2012).

Figure 4.3 shows the normal probability plot, the residual versus fitted value, the histogram, and the residual versus order. The normal probability graph implies that residual has close to normal distribution. There is no distinguishable trend for residual versus fitted value graph. Additionally, the histogram shape is close to a normal distribution curve. The residual versus observed order graph reveals proper randomization.

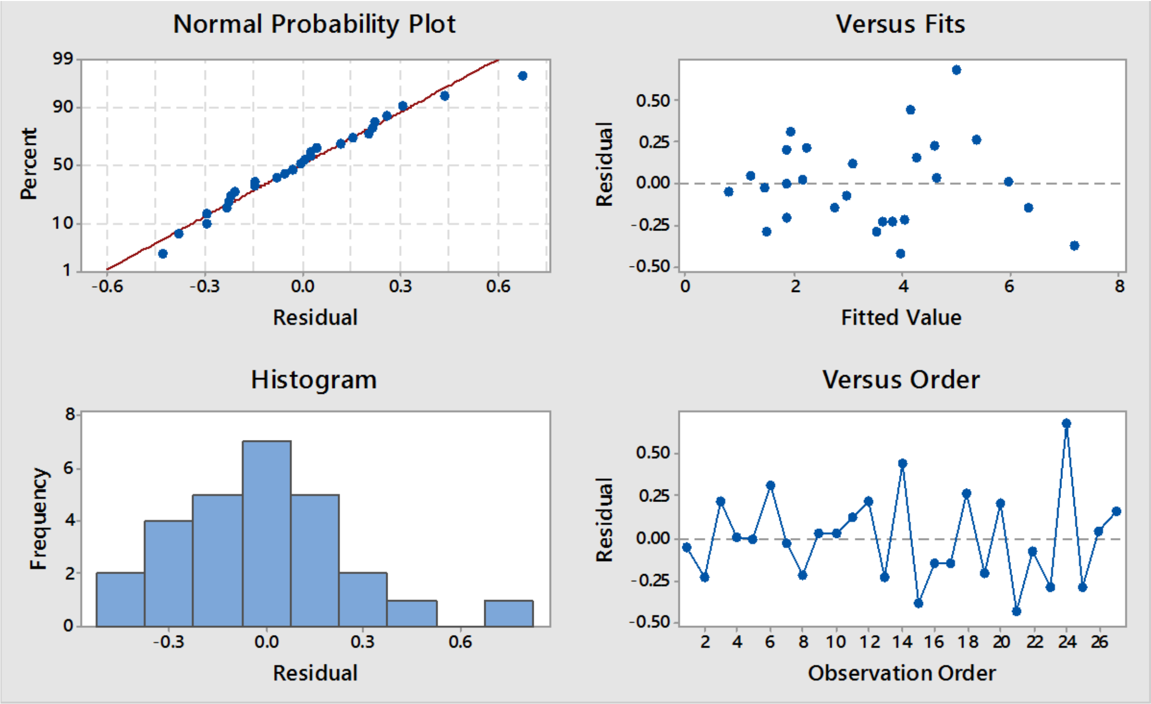

Figure 4.3-Residual plots for response (Surface roughness)

Figures 4.4 through 4.4.7 display residual versus four input factors namely laser power, laser exposure time, point distance, and remelting layer thickness. It is evident that for all independent variables of this study, constancy of variance of residual over the parameters range of study is acceptable. In addition, residual versus predicted values of dependent variable of surface roughness do not disclose any specific trend and therefore randomness of residual could be anticipated.

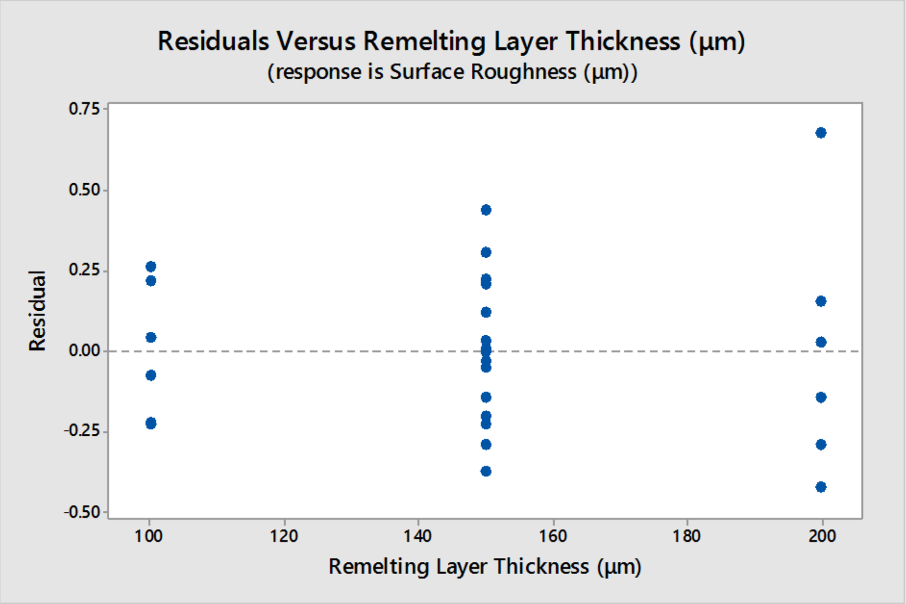

Figure 4.4-Residual versus variable T (Remelting layer thickness)

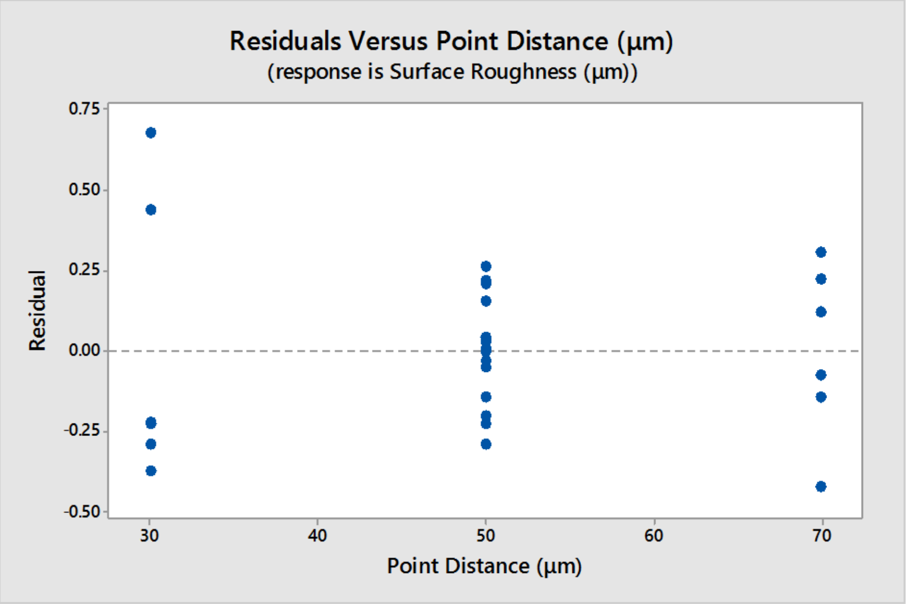

Figure 4.5-Residual versus variable D (point distance)

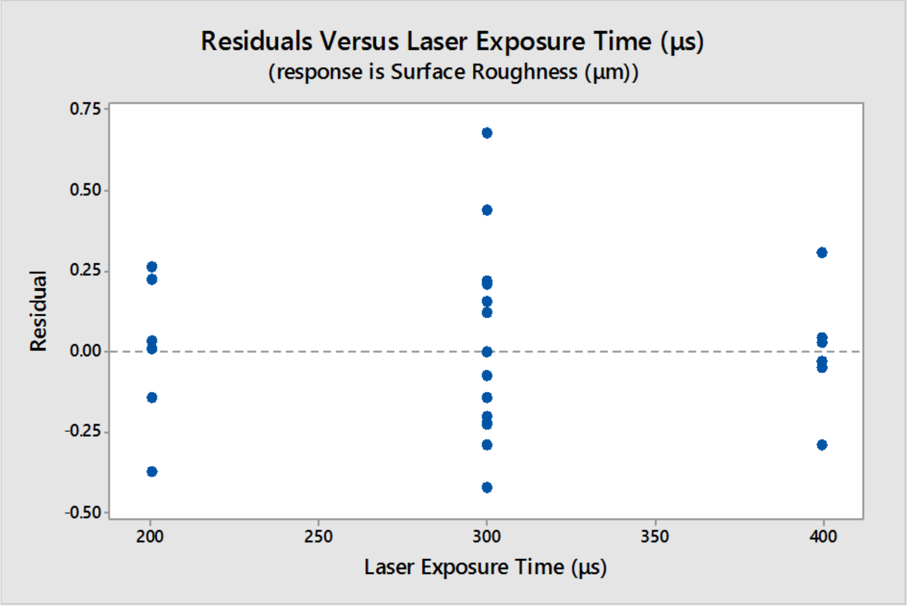

Figure 4.6-Residual versus variable E (laser exposure time)

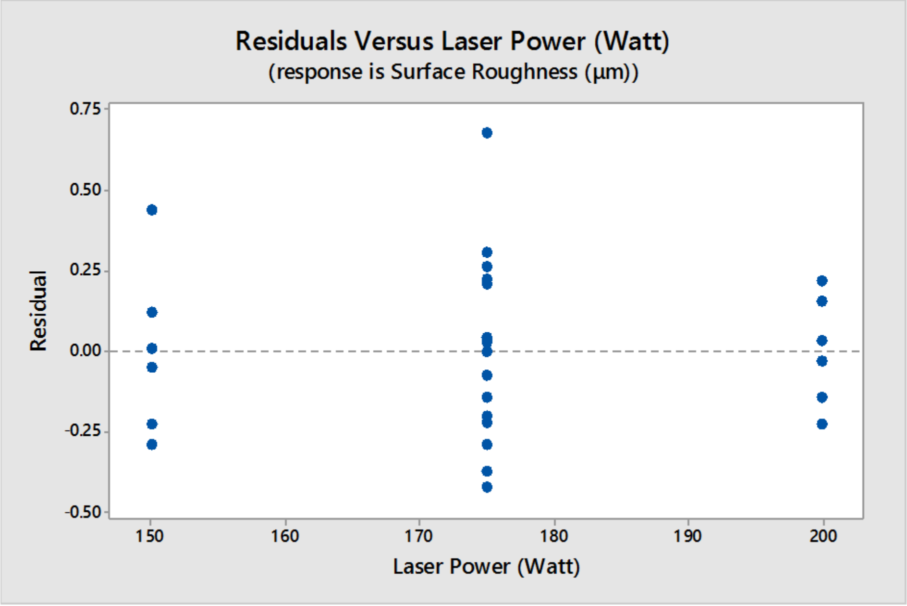

Figure 4.7-Residual versus variable P (laser power)

Figure 4.8 shows the normal probability plot of residuals. P-Value of far more than 0.05 imply that normality of residuals of predicted values appropriately are fulfilled. In other words, there is no remarkable violation of these two underlying assumptions of ANOVA analysis. Therefore, ANOVA analysis could be applied to this study data without any concern for assumptions of this statistical procedure.

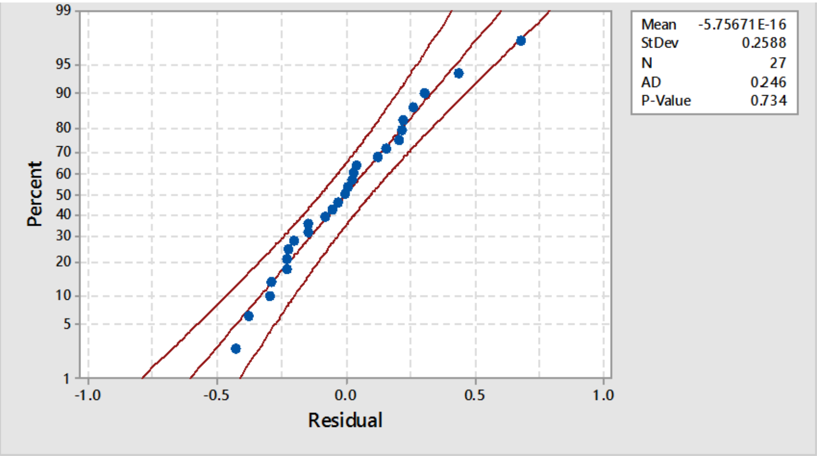

Figure 4.8- Normal probability plot of residual- 95% CI

Figure 4.9 shows fitted values versus experimental values of surface roughness. Comparing these values reveal that there is a satisfying positive relationship between calculated and measured values and proposed regression model appropriately agrees with the response variable of this study.

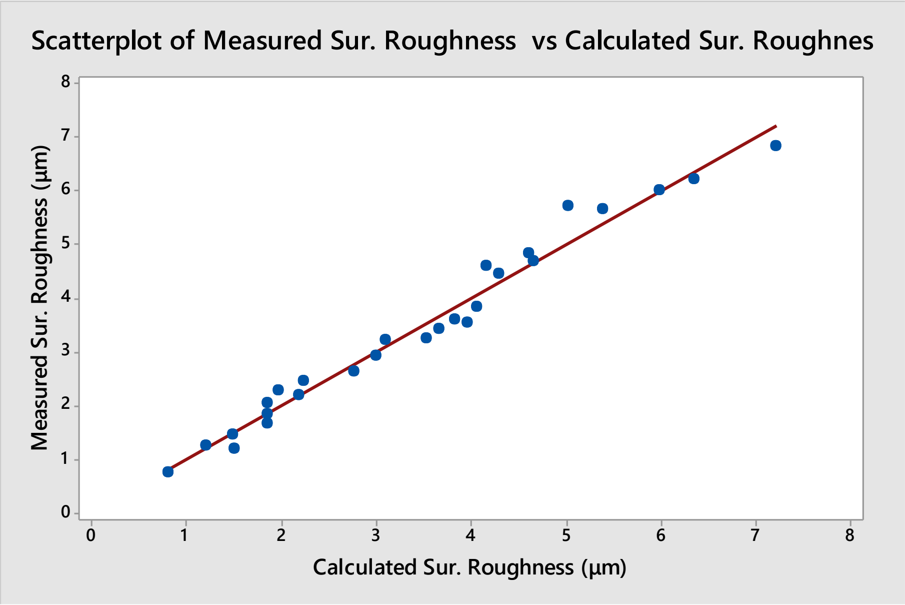

Figure 4.9- Scatter plot of surface roughness (response variable)

4.8 Contour plots of response

Figures 4.10, 4.11, and 4.12 represent six contour plot graphs for relationship between combinations of two of independent input variables (i.e. layer thickness, point distance, laser exposure time , and laser power) and surface roughness as dependent output variable. As it can be seen, contour plot is an effective tool for visualizing the effects of process input variables on the process response variable. The curvature of contours and elliptical graphs imply that process properly meets the second order model (Long et al., 2014).

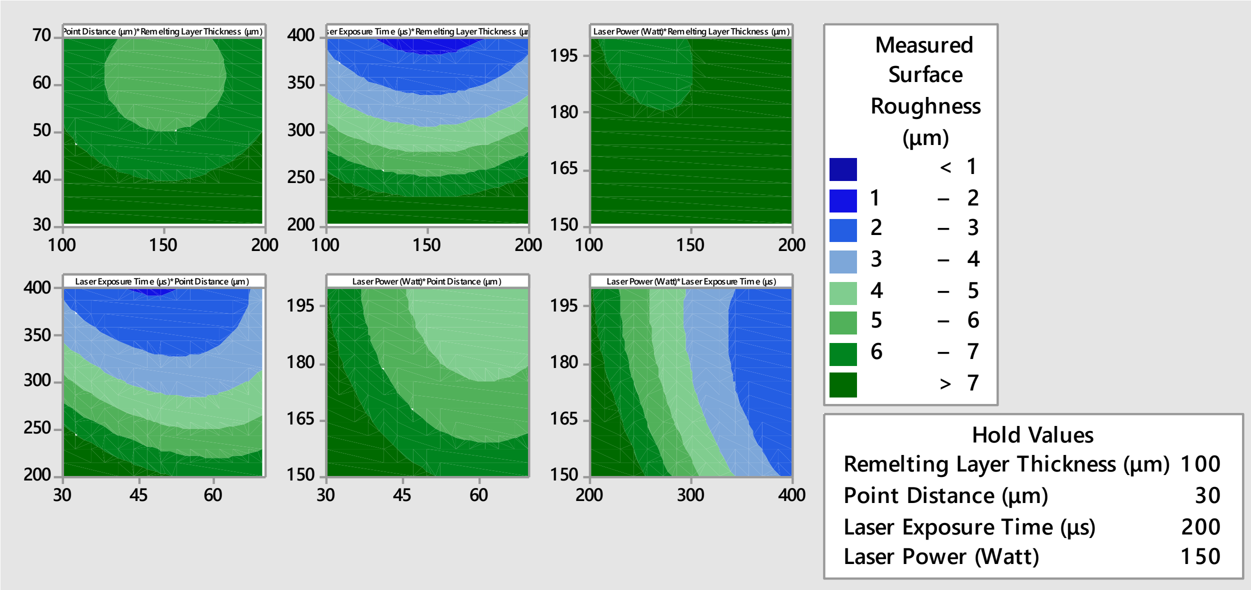

Figure 4.10- Contour plots at minimum set of hold values

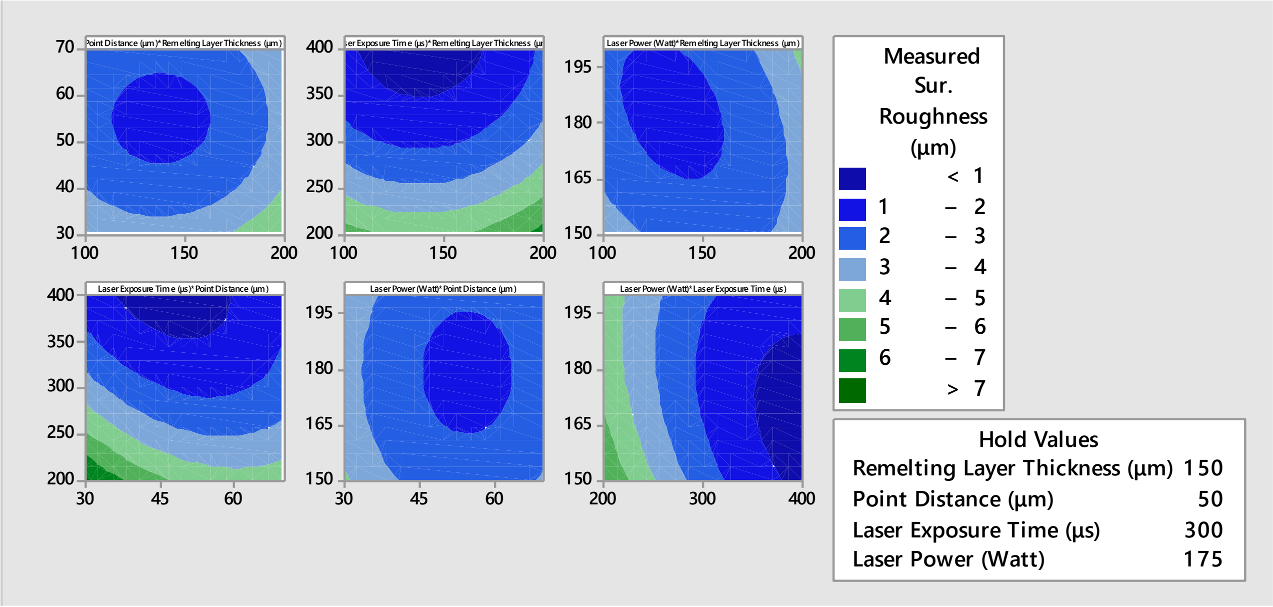

Figure 4.11- Contour plots at average set of hold values

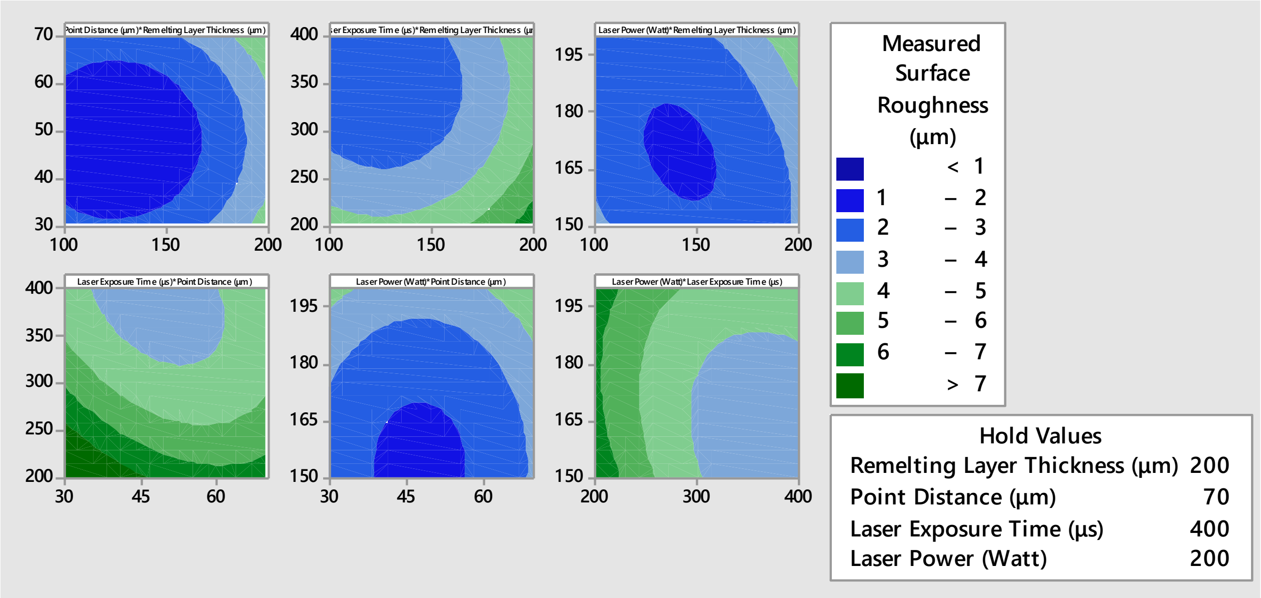

Figure 4.12- Contour plots at maximum set of hold values

Comparing contours plots at three (i.e. minimum, average, maximum) levels of hold values reveals that the optimum surface roughness at the average set of values is obtainable. The graphs of the optimum surface roughness are achievable at layer thickness of around 150 µm with laser exposure time more than 350 µs.

4.9 Surface plots of response

Similar to two-dimensional contour plots, three-dimensional surface plots also are data visualizing tools and are valuable for finding required output values and desirable operating settings. Based on the regression model for the process, each surface plot relates two independent parameters to an output parameter. It is clear that for examining the effect of two input variables on a response surface other variables of process should be held at a constant level. Figure 4.13

through 4.18 depict surface plots for four input variables of this study. Figure 4.13 shows that increasing laser exposure time remarkably improves the surface roughness. It should be noted that from process point of view there appears to be no technical limitation for increasing exposure time in order to better surface roughness.

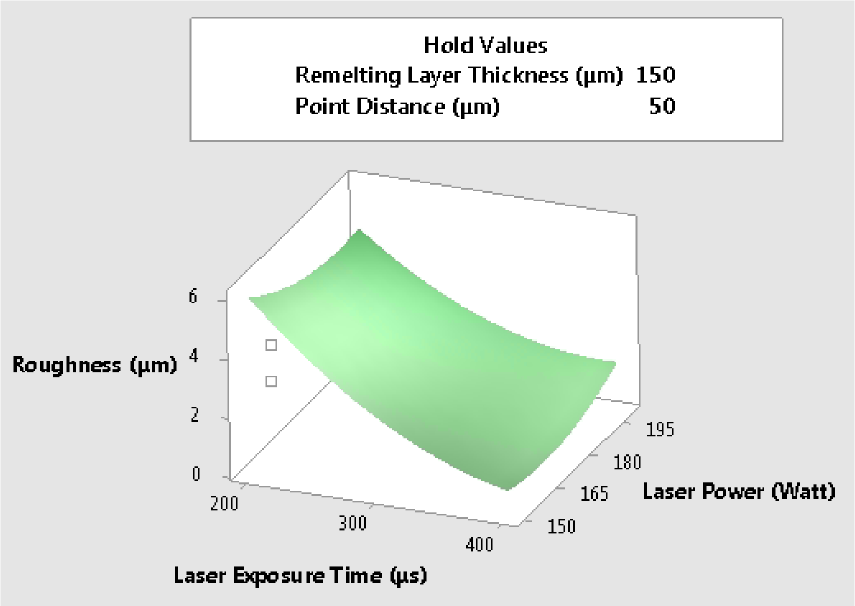

Figure 4.13- three-dimensional surface plot of surface roughness versus laser power and laser exposure time

Figure 4.14 implies that there is an optimum point distance for obtaining minimum surface roughness. As Figure 4.14 shows lower extreme of point distance has a more deterioration effect on surface roughness than the higher extreme.

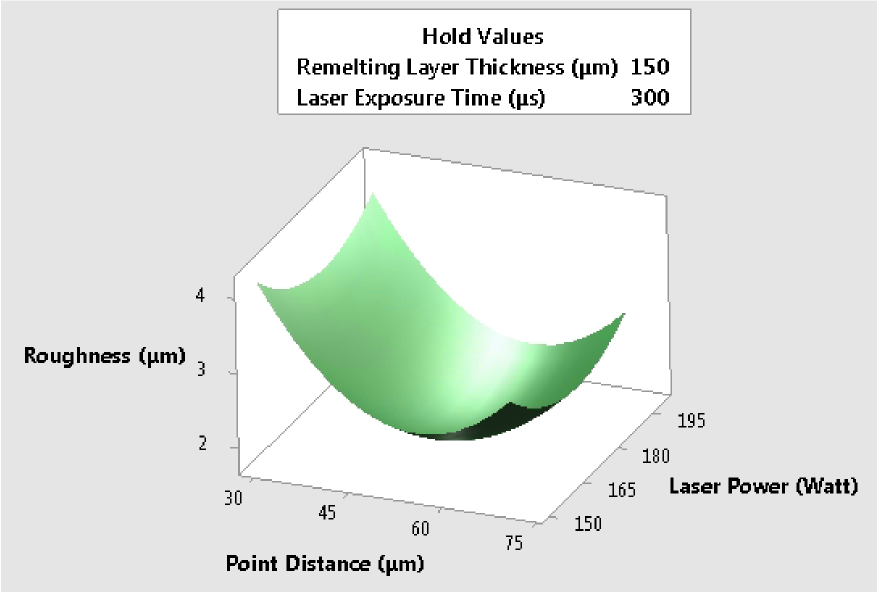

Figure 4.14- three-dimensional surface plot of surface roughness versus laser power and point distance

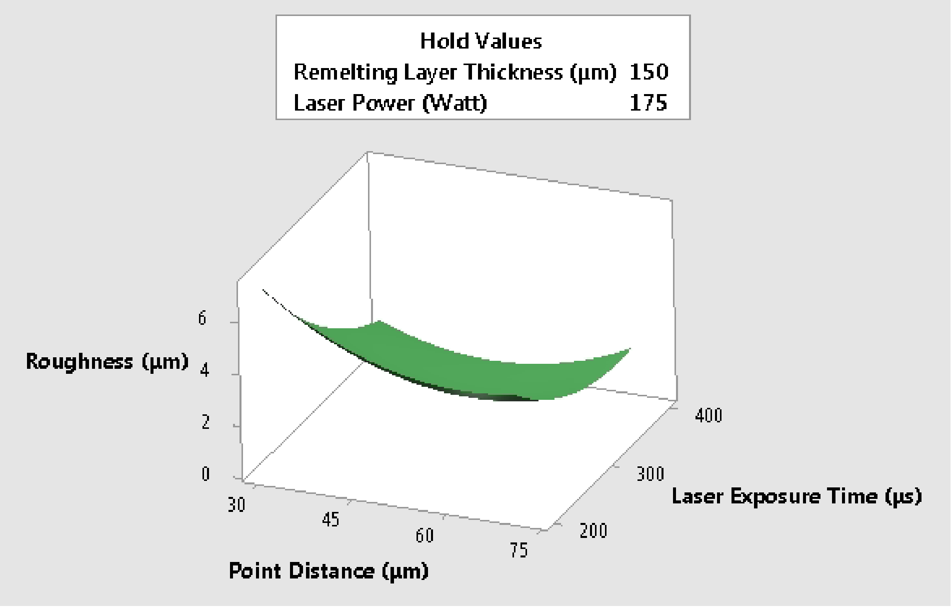

Figure 4.15- three-dimensional surface plot of surface roughness versus point distance and laser exposure time

Figure 4.16 shows that increasing layer thickness beyond about 150 µm remarkably increases the surface roughness. On the other hand, lowering layer thickness increases the remelting process time. Therefore, based on process objective there is a tradeoff among layer thickness, remelting speed, and surface roughness.

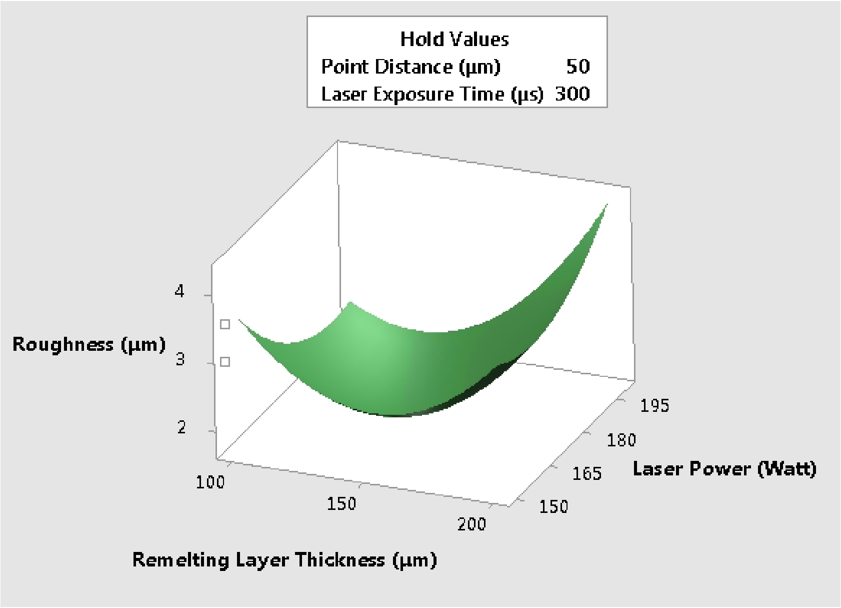

Figure 4.16- three-dimensional surface plot of surface roughness versus layer thickness and laser power

Comparison among Figures 4.13, 4.14, and 4.16 reveals the fact that for approaching optimum surface roughness, higher extreme of laser power is not required. Technically this means that current utilized AM machine is capable of providing desirable surface roughness far below maximum laser power capacity of the machine (200 Watt).

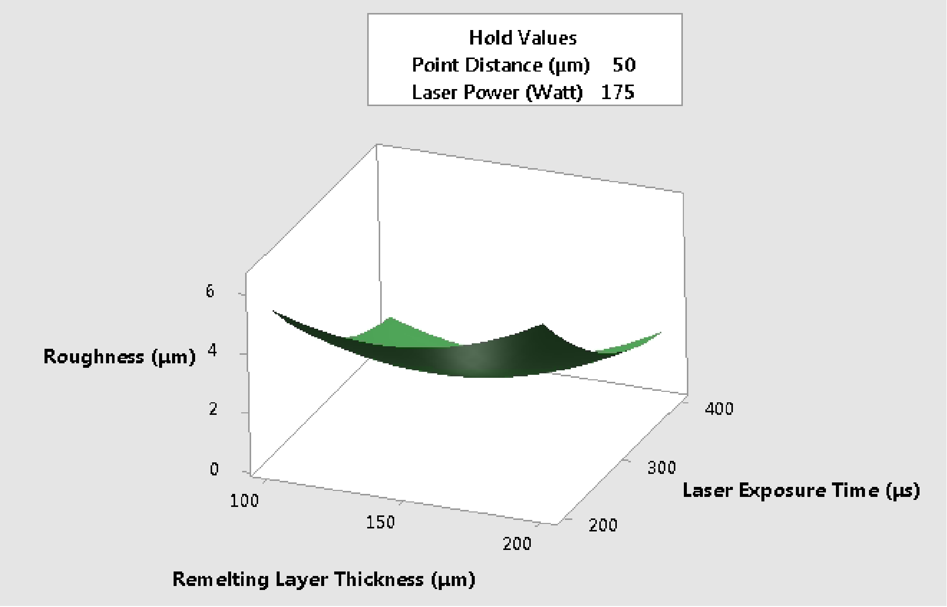

Figure 4.17- three-dimensional surface plot of surface roughness versus layer thickness and laser exposure time

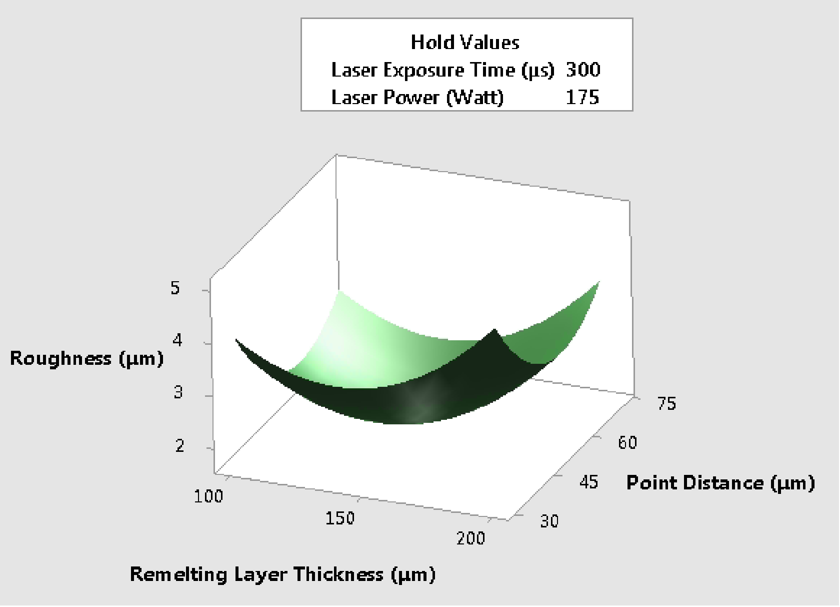

Figure 4-18-three-dimensional surface plot of surface roughness versus layer thickness and point distance

4.10 Response Optimization

Optimized set of vital input variables for obtaining optimized response is one of the ultimate objectives of RSM as a combination of statistical and mathematical tools in design of experiments approach (Akia et al, 2009). Figure 4.19 represents optimization plot of current experiment. Top of Figure displays range of input variables which are shell layer thickness (T), point distance (D), laser exposure time (E), laser power (P). As this Figure reveals, minimum (optimize for the purpose of this study) amount of surface roughness (y=0.5354) is achieved at a set of 141.41μm of shell layer thickness, 47.77 μm of point distance, 400μs of laser exposure time, and 169.19 watt of laser power. In fact, this optimization plot also represents the effect of each input parameter on the experiment response. In addition, Table 4.10 shows variable setting and fitted response for optimized prediction along with 95% CI and 95% PI. The upright red lines on the four graphs display the current input variables settings. It's worth mentioning here that these settings can be changed in order to investigate the sensitivity of surface roughness to the input variables.

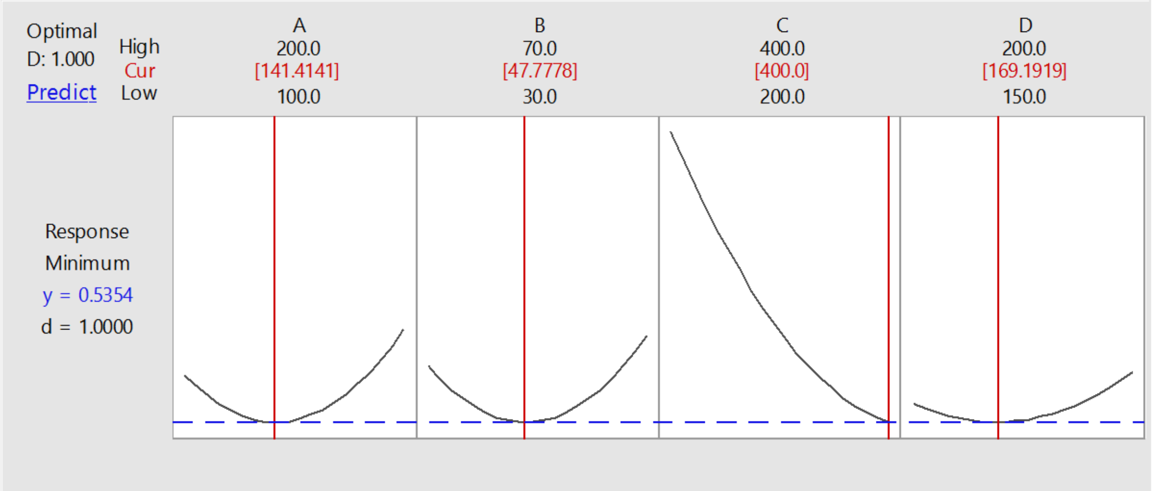

Figure 4-19- response optimization plot

Table 4.10-Variable setting and fitted response for optimized predicted solution

T	D	E	P	Response Fit	Composite Desirability	95% CI	95% PI
141.414	47.7778	400	169.192	0.535385	1	(0.153, 0.918)	(-0.285, 1.356)

4.10.1 Validation of Optimization model

In order to validate the proposed statistical optimization model, two samples were prepared according to optimal condition of process parameters. Optimal condition of parameters are 140 µm for remelting layer thickness, 50 µm for point distance, 400 µs for laser exposure time, and 170 watt for remelting laser power. At these levels of remelting process parameters, predicted surface roughness should be 0.54 µm. However, average of measured surface roughness on two prepared samples was 0.68 µm. This means that there is less than 15% difference between calculated and measured response and measured response located within 95% confidence interval.

4.11 SEM of surface

Examining surface of additive manufacturing printed parts both before and after remelting is helpful for understanding the efficiency and mechanisms of remelting process. Figures 4-20 and 4-21 show SEM images of two SLM printed samples both before and after remelting at a magnification of about 100X for run 4 and run 1 of this set of experiments. In addition, Figures 4-

22 and 4-23 show SEM images of two SLM printed samples both before and after remelting at a magnification of 400X for run 4 and run 1 of this set of experiment respectively. As these four SEM images reveal, laser remelting process on inclined surfaces has the ability to reduce irregularity of SLM prepared surface remarkably. In addition, comparing Figures 4.22 and 4.23 indicate that remelting efficiency for improving surface roughness is highly influenced by process parameters. In other words, optimization of selective laser remelting process parameters play crucial rule in effective application of this process (Cherry et al., 2015).

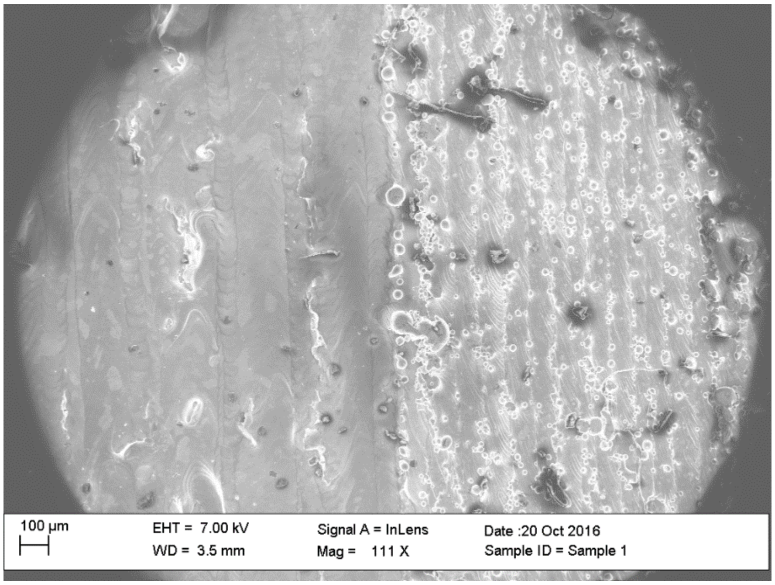

Figure 4-20- SEM image of run 4 sample at magnification 100 (Remelting layer thickness: 150 µm, Point distance: 50 µm, Laser exposure time: 200 µs, Laser power: 150 Watt)

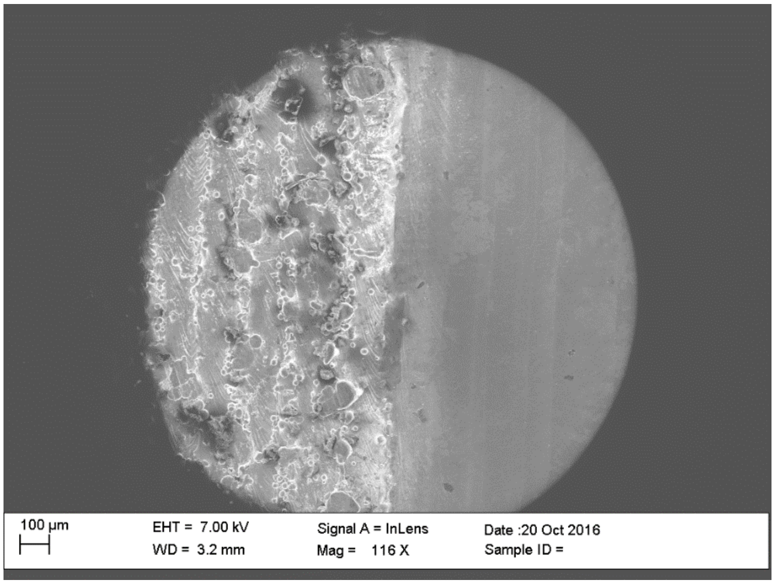
100 µm
EHT = 7.00 kV
WD = 3.2 mm
Signal A = InLens
Mag = 116 X
Date :20 Oct 2016
Sample ID =

Figure 4-21- SEM image of run 1 sample at magnification 100 (Remelting layer thickness: 150 µm, Point distance: 50 µm, Laser exposure time: 400 µs, Laser power: 150 Watt)

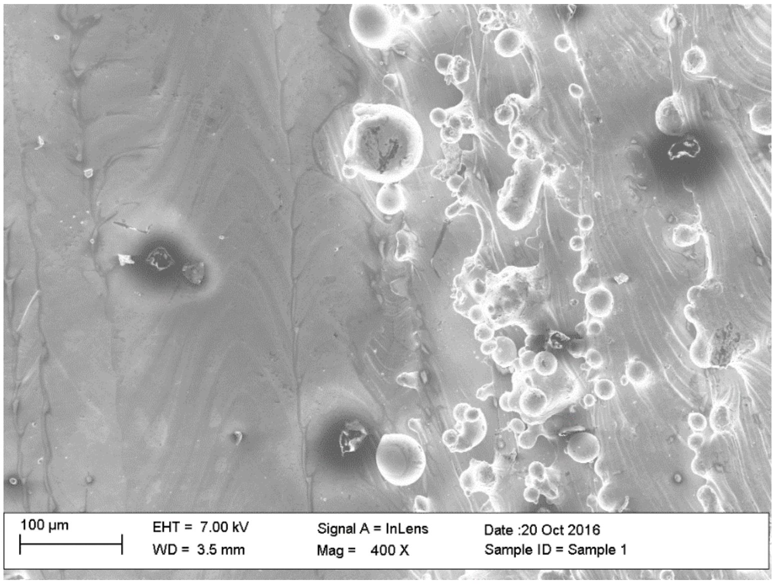
100 µm
EHT = 7.00 kV
WD = 3.5 mm
Signal A = InLens
Mag = 400 X
Date :20 Oct 2016
Sample ID = Sample 1

Figure 4-22- SEM image of run 4 sample at magnification 400 (Remelting layer thickness: 150 µm, Point distance: 50 µm, Laser exposure time: 200 µs, Laser power: 150 Watt)

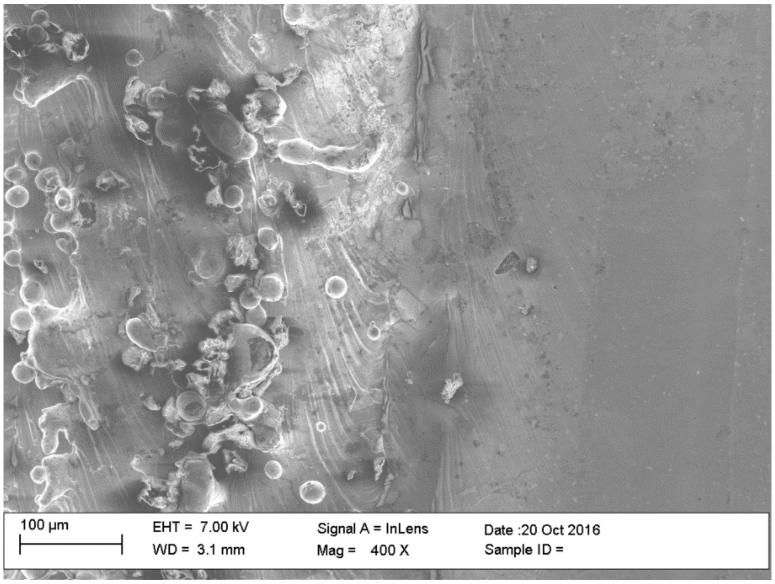
100 µm
EHT = 7.00 kV
WD = 3.1 mm
Signal A = InLens
Mag = 400 X
Date :20 Oct 2016
Sample ID =

Figure 4-23- SEM image of run 1 sample at magnification 400 (Remelting layer thickness: 150 µm, Point distance: 50 µm, Laser exposure time: 400 µs, Laser power: 150 Watt)

Figure 4.24 shows at least two adjacent laser paths on two consecutive remelting layers. In contrary to a previous publication (Yasa and Kruths, 2011), this result reveals that with optimized selection of process parameters, roughness in overlap area also could be improved significantly.

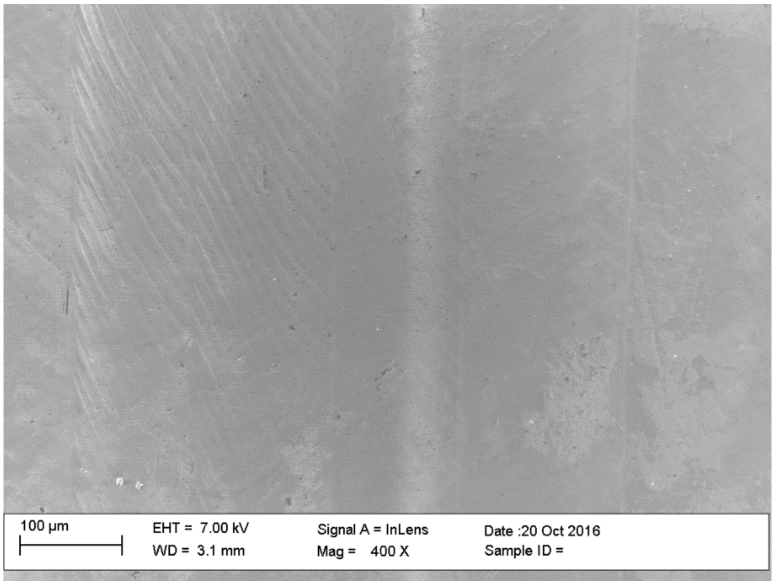
100 µm
EHT = 7.00 kV
WD = 3.1 mm
Signal A = InLens
Mag = 400 X
Date :20 Oct 2016
Sample ID =

Figure 4-24- SEM image of central area of run 1 sample at magnification 400 (Remelting layer thickness: 150 µm, Point distance: 50 µm, Laser exposure time: 400 µs, Laser power: 150 Watt)

CHAPTER V

CONCLUSIONS AND FUTURE RESEARCH

Over the last decade additive manufacturing has increasingly been used for customized manufacturing of functional parts, in particular, for aerospace and biomedical industries. There is a massive driving force to widen AM application in other industries including automotive. In spite of the variety of advantages, AM technologies still have some real challenges. One of these challenges is to achieve desirable surface roughness. In fact, this characteristic is highly important for functional parts which work under dynamic loads. This research is truly an attempt to improve the surface roughness in SLM process. Conclusions of this research are summaries as follows:

1-Improving inclined surface roughness of 316L stainless steel below 1 µm by a hybrid SLM and remelting process is feasible.

2-For remelting of inclined surfaces, laser exposure time plays the most important role in obtaining low surface roughness.

3-The results reveal that hatch distance has no effect on inclined surface remelting but there is an optimal value for layer thickness for the remelting process. Layer thickness of 50 µm and 100 µm widely are used for selective laser melting of 316L stainless steel, however, for consecutive laser remelting a layer thickness of 200 µm could be applied. In other words, production rate of laser remelting on inclined surfaces can be twice the selective laser melting process.

4-This study mainly focused on remelting of 45º inclined surfaces. Optimization of remelting process parameters for other (lower and higher) inclined angles could also be investigated and optimized.

5-Currently, the substrate is fixed and just moves in Z direction in the SLM system. However for remelting of geometrically complex parts, giving more degrees of freedom and rotation to the substrate should be investigated.

REFERENCES

Ahn, D., Kimb, H., & Lee, S. (2009). Surface roughness prediction using measured data and interpolation in layered manufacturing. Journal of materials processing technology, 209, 664–671.

Akia, M., Alavi, S.M., Rezaei, M., Zi-Feng Yan Z. (2009).Optimizing the sol–gel parameters on the synthesis of mesostructured nanocrystalline γ-Al2O3. Microporous and Mesoporous Materials, 122, 72–78

Alrbaey, K., Wimpenny, D., Tosi, R., Manning, W., & Moroz, A. (2014). On Optimization of Surface Roughness of Selective Laser Melted Stainless Steel Parts: A Statistical Study. Journal of Materials Engineering and Performance, 23, 2139–2148.

Bordatchev, E.V., Hafiz, A.M.K. & Tutunea-Fatan, O.R. (2014) .Performance of laser polishing in finishing of metallic surfaces. The International Journal of Advanced Manufacturing Technology, 73, 35–52.

Boschetto, A., & Bottini, L. (2015). Roughness prediction in coupled operations of fused deposition modeling and barrel finishing . Journal of Materials Processing Technology, 219, 181–192.

Bourell, D.L. (2016). Perspectives on Additive Manufacturing. Department of Mechanical Engineering, the University of Texas, Austin, Texas.

Braga,F.J.C., Marques, R.C.M., Filho, E.D.A., & Guastaldi, A.C. (2007). Surface modification of Ti dental implants by Nd:YVO4 laser irradiation. Applied Surface Science, 253, 9203–9208.

Cherry, J.A., Davies, H.M., Mehmood, S., Lavery, N.P., Brown, S.G.R. & J. Sienz, J. (2015).Investigation into the effect of process parameters on microstructural and physical properties of 316L stainless steel parts by selective laser melting. International Journal of Advanced Manufacturing Technology,76, 869–879

Chu,WS., Kim, CS., & Lee, HT. (2014). Hybrid Manufacturing in Micro/Nano Scale: A Review, International Journal of precision engineering and manufacturing green technology, 1, 75-92.

Frazier, W.E. (2014). Metal Additive Manufacturing: A Review, Journal of Materials Engineering and Performance. 23, 1917-1928.

Gibson, I., Rosen, D.W., & Stucker, B. (2014).Additive Manufacturing Technologies: Rapid Prototyping to Direct Digital Manufacturing. Springer, New York.

Gu, D.D., Meiners,W., Wissenbach, K. , & Poprawe, R. (2012). Laser additive manufacturing of metallic components: materials, processes and mechanisms. International Materials Reviews, 57, 3, 133-164.

Hamze, H., Mandana Akia, A, & Yazdani, F. (2015). Optimization of biodiesel production from the waste cooking oil using response surface methodology. Process Safety and Environmental Protection 94, 1–10

Herzog, D., Seyda, V. Wycisk, E., & Emmelmann, C. (2016). Additive manufacturing of metals. Acta Materialia, 117, 371–392.

Jia, Q., & Gu, D. (2014). Selective laser melting additive manufacturing of Inconel 718 superalloy parts: Densification, microstructure and properties. Journal of Alloys and Compounds, 585, 713–721.

Kamath, C., El-dasher, B., Gallegos, G.F., King, W. E., & Sisto, A., (2014). Density of additively-manufactured, 316L SS parts using laser powder-bed fusion at powers up to 400 W. The International Journal of Advanced Manufacturing Technology, 74, 65-78.

Karunakaran, K.P., Suryakumar, S., Pushpa, V., & Akula, S. (2010). Low cost integration of additive and subtractive processes for hybrid layered manufacturing. Robotics and Computer-Integrated Manufacturing, 26, 490–499.

King , W.E., Barth, H. D. , Castillo, V. M. , Gallegos, G.F., Gibbs, J. W. , Hahn, D. E., Kamath, C., & Rubenchik, A. M. (2014). Observation of keyhole-mode laser melting in laser powder-bed fusion additive manufacturing. Journal of Materials Processing Technology, 214, 2915–2925.

Kruth, J.P.,Yasa, E., & Deckers, J. (2008). Roughness Improvement in Selective Laser Melting. Proceedings of the 3rd International Conference on Polymers and Moulds Innovations, 170-183. Journal of Materials Processing Technology, 232, 1–8.

Lamikiz, A., Sánchez, J.A., López de Lacalle, L.N., & Arana, J.L. (2007). Laser polishing of parts built up by selective laser sintering. International Journal of Machine Tools and Manufacture, 47, 2040–2050.

Lauwers, B. , Klocke , F., Klink, A., Tekkaya, A.E. , Neugebauer, R., & Mcintosh, D. (2014). Hybrid processes in manufacturing. CIRP Annals - Manufacturing Technology, 63, 561–583.

Lavvafi, H., Lewandowski, J., Dudzinski, D., & Lewandowski, J.J. (2012). Effects of ultrafast laser micromachining on structure and mechanical properties of 316 LVM Stainless Steel. AIP Conference Proceedings, American Institute of Physics, Ste. 1 NO 1 Melville NY, 11747-4502, United States.

Lavvafi, H. (2013). Effects of laser machining on structure and fatigue of 316LVM biomedical wires. Dissertation, Case Western Reserve University.

Li, J., Gonzalez, M.A., & Zhu, Y. (2009). A hybrid simulation optimization method for production planning of dedicated remanufacturing. Int. J. Production Economics, 117, 286–301

Löber, L., Flache,C., Petters, R., Kühn, U., Jürgen Eckert, J.(1995). Comparison of different post processing technologies for SLM generated 316l steel parts. Rapid Prototyping Journal, 19, 173 – 179.

Long, Y., Li, J., Timmer, D., Jones, R.E., & Gonzalez, M.A. (2014). Modeling and optimization of the molten salt cleaning process. Journal of Cleaner Production, 68 243-251

Merklein , M., Junker, D., Schaub, A., & Neubauer, F. (2016). Hybrid Additive Manufacturing Technologies – An Analysis Regarding Potentials and Applications. Physics Procedia, 83, 549–559.

Mognol, P., Jégou, L., Rivette, M., & Furet, B. (2006). High speed milling, electro discharge machining and direct metal laser sintering: A method to optimize these processes in hybrid rapid tooling. The International Journal of Advanced Manufacturing Technology, 29, 35–40.

Montgomery, D.C., (2012). Design and Analysis of Experiments. Wiley, ISBN-10: 1118146921

Montgomery, D.C., Peck, E.A., & Vining, G.G. (2006). Introduction to Linear Regression Analysis 4th Edition, Wiley-Interscience, ISBN-10: 0471754951

Mumtaz, K., & Hopkinson, N., (2009).Top surface and side roughness of Inconel 625 parts processed using selective laser melting. Rapid Prototyping Journal, 15, 96 – 103.

Osborne, J.W., (2010).Improving your data transformations: Applying the Box-Cox transformation. Practical assessment, Research & Innovation, 15, 12,

Park, J.W., & Lee, D.W. (2009). Pulse electrochemical polishing for microrecesses based on a coulostatic analysis. The International Journal of Advanced Manufacturing Technology, 40, 742–748.

Rosal, B., Mognol, P., & Hascoët, J.Y. (2015). Laser polishing of additive laser manufacturing surfaces. Journal of Laser Applications, 27 1-7.

Singhal, S.K. Jain, P.K., Pandey, P.M. & Nagpal, A.K. (2009). Optimum part deposition orientation for multiple objectives in SL and SLS prototyping. International Journal of Production Research, 47, 6375-6396.

Strano, G., Hao, L, Everson, R.M., & Evans, K.E. (2013). Surface roughness analysis, modelling and prediction in selective laser melting. Journal of Materials Processing Technology, 213, 589–597.

Vaithilingama, J., Goodridgea, R.D., Haguea, R.J.M., Christieb, S.D.R., Edmondson, S. (2016). The effect of laser remelting on the surface chemistry of Ti6al4V components fabricated by selective laser melting.

Wang, D., Liu, Y., Yang, Y., & Xiao, D., (2016).Theoretical and experimental study on surface roughness of 316L stainless steel metal parts obtained through selective laser melting. Rapid Prototyping Journal, 22 , 706 – 716

Wang, D., Mai, S., Xiao, D. & Yang, Y. (2016).Surface quality of the curved overhanging structure manufactured from 316-L stainless steel by SLM. International Journal of advanced Manufacturing Technology , 86,781–792

Wu, Z., Li, J., Timmer T., Karen Lozano, K., & Bose, S. (2009). Study of processing variables on the electrical resistivity of conductive adhesives. International Journal of Adhesion & Adhesives 29 (2009) 488–494

Yadroitsev, I., Bertrand, P., & Smurov, I. (2007). Parametric analysis of the selective laser melting process. Applied Surface Science, 253, 8064–8069.

Yasa, E., Deckers, J., & Kruth, J.P. (2011). The investigation of the influence of laser re-melting on density, surface quality and microstructure of selective laser melting parts. Rapid Prototyping Journal, 17, 312 – 327.

Yasa, E. & Kruth, J. (2011). Application of laser remelting on selective laser melting parts. Advances in Production Engineering & Management, 6, 259-270.

Yasa, E. & Kruth, J-P. (2011). Microstructural investigation of Selective Laser Melting 316L stainless steel parts exposed to laser re-melting. Procedia Engineering, 19, 2011, 389-395.

Yoon, H.S., Lee, J.Y., Kim, H.S., Kim, M.S., Kim, E.S., Shin, Y.J., Chu, W.S., & Ahn, S.H. (2014). A comparison of energy consumption in bulk forming, subtractive, and additive processes: Review and case study. International Journal of Precision Engineering and Manufacturing-Green Technology, 1, 3, 261–279.

BIOGRAPHICAL SKETCH

Jafar Ghorbani was born on July 11th, 1976 in Semirom, Iran. He entered the Isfahan University of Technology (One of the top 3 nationwide University) in 1995 and earned a bachelor degree in Materials Engineering in 1999. Then he moved to the University of Tehran (One of the top 3 nationwide University) and graduated in 2002 with a master degree in Materials Engineering (emphasis on characterization, selection and design of engineering materials). Topic of his thesis at university of Tehran was fatigue of vanadium micro alloyed steels and its results published in more than 6 national and international conference and journal papers.

From 2003 to 2014 Jafar worked for several companies mainly in energy sectors at welding inspector, welding engineer, materials engineer and quality lead positions. In January 2015 he moved to USA to pursue his education in manufacturing engineering programs at the University of Texas-Pan American. (UTPA). When he enrolled as a graduate student, he had the opportunity to be a graduate assistant for the Manufacturing& Industrial Engineering department at UTRGV where he worked for three semesters. Jafar earned his master degree in manufacturing engineering from UTRGV in December 2016. Jafar's email address is Ghorbani_jafar@yahoo.com.